

Non-Stationary Online Structured Prediction with Surrogate Losses

Shinsaku Sakaue

CyberAgent, National Institute of Informatics, RIKEN AIP

shinsaku.sakaue@gmail.com

Han Bao

The Institute of Statistical Mathematics, Tohoku University

bao.han@ism.ac.jp

Yuzhou Cao

Nanyang Technological University

nanjing.caoyuzhou@gmail.com

Abstract

Online structured prediction, including online classification as a special case, is the task of sequentially predicting labels from input features. Therein the *surrogate regret*—the cumulative excess of the target loss (e.g., 0-1 loss) over the surrogate loss (e.g., logistic loss) of the fixed best estimator—has gained attention, particularly because it often admits a finite bound independent of the time horizon T . However, such guarantees break down in *non-stationary* environments, where every fixed estimator may incur the surrogate loss growing linearly with T . We address this by proving a bound of the form $F_T + C(1 + P_T)$ on the cumulative target loss, where F_T is the cumulative surrogate loss of any comparator sequence, P_T is its *path length*, and $C > 0$ is some constant. This bound depends on T only through F_T and P_T , often yielding much stronger guarantees in non-stationary environments. Our core idea is to synthesize the dynamic regret bound of the online gradient descent (OGD) with the technique of *exploiting the surrogate gap*. Our analysis also sheds light on a new Polyak-style learning rate for OGD, which systematically offers target-loss guarantees and exhibits promising empirical performance. We further extend our approach to a broader class of problems via the *convolutional Fenchel-Young loss*. Finally, we prove a lower bound showing that the dependence on F_T and P_T is tight.

1 Introduction

In supervised learning, the goal is to predict the ground-truth label $y \in \mathcal{Y}$ corresponding to an input vector $\mathbf{x} \in \mathcal{X}$. For example, the K -class classification problem asks to predict a label in $\mathcal{Y} = \{1, \dots, K\}$. In more involved problems, a label may represent a complex structured object, such as a matching or a tree. Such problems are collectively known as *structured prediction*, which has been extensively studied and applied to various fields including natural language processing and bioinformatics [1].

This paper studies the sequential version of structured prediction, where a learner and an environment sequentially interact over T rounds. At each round t , the learner observes an input $\mathbf{x}_t \in \mathcal{X}$ and makes a prediction $\hat{y}_t \in \hat{\mathcal{Y}}$, where $\hat{\mathcal{Y}}$ denotes the set of predictions. The environment then reveals ground-truth $y_t \in \mathcal{Y}$, and the learner incurs a target loss of $\ell(\hat{y}_t, y_t)$, which measures the discrepancy between \hat{y}_t and y_t . The learner’s goal is to minimize the cumulative target loss over T rounds, i.e., $\sum_{t=1}^T \ell(\hat{y}_t, y_t)$. A well-known example is online classification, where $\mathcal{Y} = \hat{\mathcal{Y}} = \{1, \dots, K\}$ and the target loss is the 0-1 loss.

In many structured prediction problems, the label set \mathcal{Y} is discrete, which prevents us from learning direct mappings from \mathcal{X} to \mathcal{Y} via efficient continuous optimization methods. A standard workaround is to adopt the surrogate loss framework (see e.g., [2]). Specifically, we define an intermediate score space \mathbb{R}^d between

\mathcal{X} and \mathcal{Y} and a surrogate loss $L(\boldsymbol{\theta}_t, y_t)$,¹ which quantifies how well the score vector $\boldsymbol{\theta}_t \in \mathbb{R}^d$ is aligned with ground-truth $y_t \in \mathcal{Y}$. With this framework, we can efficiently learn mappings from \mathcal{X} to \mathbb{R}^d via continuous optimization. Following prior work [31, 32, 28, 29], we focus on learning linear estimators $\mathbf{W}_t: \mathcal{X} \rightarrow \mathbb{R}^d$ over $t = 1, \dots, T$, where each \mathbf{W}_t computes a score vector as $\boldsymbol{\theta}_t = \mathbf{W}_t \mathbf{x}_t$. We make a prediction $\hat{y}_t \in \hat{\mathcal{Y}}$ from the score vector $\boldsymbol{\theta}_t \in \mathbb{R}^d$ via a mapping, called *decoding*, from \mathbb{R}^d to $\hat{\mathcal{Y}}$, which depends on the problem setting as detailed in Sections 3.1 and 4.1.

In online structured prediction with the surrogate loss framework, a widely used performance measure is the following *surrogate regret*, denoted by R_T :

$$\sum_{t=1}^T \ell(\hat{y}_t, y_t) = \sum_{t=1}^T L(\mathbf{U} \mathbf{x}_t, y_t) + R_T, \quad (1)$$

where \mathbf{U} is the best offline linear estimator minimizing the cumulative surrogate loss.² In words, the surrogate regret R_T represents the learner's extra target loss compared to the best offline performance within the surrogate loss framework. Since Van der Hoeven [31] explicitly introduced the surrogate regret in online classification, follow-up studies have adopted this measure and extended it to structured prediction [32, 28, 29]. Notably, this line of work has achieved finite surrogate regret bounds, which ensure that R_T is upper bounded independently of T , under full-information feedback (i.e., $y_t \in \mathcal{Y}$ is revealed).³ This is an elegant extension of the classical finite mistake bound of the perceptron for linearly separable binary classification [27], where the hinge loss $L(\mathbf{U} \mathbf{x}_t, y_t)$ takes zero under separability (see e.g., [23, Section 8.2]).

However, finite surrogate regret bounds may fall short in non-stationary environments. To illustrate with an intuitive example, consider an online binary classification instance that is linearly separable for the first $T/2$ rounds, but then all labels are flipped for the remaining $T/2$ rounds. In this scenario, no fixed offline estimator \mathbf{U} can avoid incurring a cumulative surrogate loss of $\sum_{t=1}^T L(\mathbf{U} \mathbf{x}_t, y_t) = \Omega(T)$. Consequently, even though R_T is finite, the upper bound on the cumulative target loss, $\sum_{t=1}^T \ell(\hat{y}_t, y_t)$, grows linearly with T , rendering the guarantee meaningless. Is it then possible to obtain upper bounds on the cumulative target loss that do not grow linearly with T even in non-stationary settings?

1.1 Our Contribution

This paper focuses on the full-information online structured prediction and establishes the following bound on the cumulative target loss:

$$\sum_{t=1}^T \ell(\hat{y}_t, y_t) = F_T + c(1 + P_T), \quad (2)$$

where $F_T = \sum_{t=1}^T L(\mathbf{U}_t \mathbf{x}_t, y_t)$, $P_T = \sum_{t=2}^T \|\mathbf{U}_t - \mathbf{U}_{t-1}\|_F$ ($\|\cdot\|_F$ denotes the Frobenius norm) for any comparator sequence $\mathbf{U}_1, \dots, \mathbf{U}_T$, and $c > 0$ denotes a problem-dependent constant. In non-stationary environments, this bound can offer significantly stronger guarantees than previous bounds of the form (1). For example, in the aforementioned non-stationary binary classification instance, we can set \mathbf{U}_t to the best offline linear estimator for the first $T/2$ rounds and to its negative for the latter $T/2$ rounds, which yields $F_T = 0$ for surrogate losses with a separation margin (e.g., the smooth hinge loss) and $P_T = O(1)$, achieving $\sum_{t=1}^T \ell(\hat{y}_t, y_t) = O(1)$. This is far better than $\sum_{t=1}^T \ell(\hat{y}_t, y_t) = \Omega(T)$ implied by the existing finite bounds on R_T in (1). Regret bounds that depend on F_T is called *small-loss* bounds [11, 36], and the quantity P_T is called the *path length* [37]. Thus, we call a bound of the form (2) a “small-surrogate-loss + path-length” bound. Note that our bound (2) generalizes the finite bound on R_T in (1) since setting $\mathbf{U}_1, \dots, \mathbf{U}_T$ to the best offline \mathbf{U} achieves $P_T = 0$.

Similar to prior work [31, 32, 28, 29], our approach consists of two parts: online convex optimization (OCO) for surrogate losses and decoding of estimated score vectors. We use the online gradient descent (OGD)

¹While we focus on the Euclidean score space, a general framework on Hilbert spaces is also studied [12, 13].

²We write $\sum_{t=1}^T L(\mathbf{U} \mathbf{x}_t, y_t)$ on the right-hand side to clarify that this is not a proper regret, following Van der Hoeven et al. [32].

³Another common setting is bandit feedback, where only $\ell(\hat{y}_t, y_t) \in \mathbb{R}$ is revealed.

for the OCO part, while we employ decoding methods of the previous studies. Our technical innovation lies in a simple yet effective idea for synthesizing the dynamic regret analysis of Zinkevich [37], who showed that OGD enjoys a regret bound of $O(\sqrt{T}(1 + P_T))$ in OCO, with a so-called *surrogate gap* arising from the decoding process (see Section 3). This idea further provides an insight for designing a new Polyak-style learning rate, which systematically provides guarantees on the target loss and delivers favorable empirical performance.

In Section 4, we tackle a significantly broader range of structured prediction problems beyond the scope of prior work, which includes, for example, label ranking with different label and prediction sets (see Appendix A.3). This is achieved with a recent surrogate loss framework, called the *convolutional Fenchel–Young loss*, proposed by Cao et al. [10]. This framework is useful as it provides a principled way to construct desirable smooth surrogate losses based on target-loss structures. We introduce new technical tools for convolutional Fenchel–Young losses, which, combined with our main strategy in Section 3, enable us to establish the bound in (2) for the broader class of problems.

Finally, Section 5 presents a lower bound to show that the dependence on F_T and P_T is tight. This result suggests an interesting side observation: in online structured prediction, the classical approach of Zinkevich [37] suffices to obtain the bound in (2) that is tight in terms of F_T and P_T , while recent work provides improved dynamic regret bounds in OCO [34, 35, 36], as detailed in Section 1.2.

1.2 Related Work

Structured prediction. We discuss particularly relevant studies on structured prediction; see, e.g., Sakaue et al. [28, Appendix A] for a comprehensive overview. Our work is based on an inner-product representation of target losses, as detailed in Section 2.1. One such well-known framework is the *structure encoding loss function* [12, 13], and we adopt its extensions studied by Blondel [5] and Cao et al. [10]. Regarding surrogate losses, our scope mainly covers, but not limited to, *Fenchel–Young losses*, proposed by Blondel et al. [7] (see Section 2.2). Also, our approach in Section 4 is based on the convolutional Fenchel–Young loss, proposed by Cao et al. [10]. This surrogate loss framework provides a nice family of smooth surrogate losses such that the surrogate excess risk linearly bounds the target excess risk from above [10, Theorem 15], a remarkable property in statistical learning. Note, however, that in our online setting, “small-surrogate-loss + path-length” bounds of the form (2) cannot be derived merely by using the convolutional Fenchel–Young loss as the surrogate; new technical lemmas introduced in Section 4.2 are required.

Online classification and structured prediction. Online classification has a broad literature; we refer the reader to an excellent overview by Van der Hoeven [31, Section 1]. Of particular relevance to our work, the classical perceptron [27] enjoys a finite mistake bound in the binary case under linear separability. Van der Hoeven [31] extended this result to multiclass classification and obtained a finite surrogate regret bound (1), which holds regardless of separability. Sakaue et al. [28] extended the result to online structured prediction with Fenchel–Young losses. Prior work on online classification/structured prediction also explored various limited feedback settings [31, 32, 29], while our work, as the first step toward the non-stationary setting, focuses on full-information feedback. Addressing non-stationarity is a crucial challenge in online structured prediction. Independent of our work, Boudart et al. [8] studied non-stationary online structured prediction, but their performance metric differs from ours and their regret bounds explicitly depend on T , unlike our bounds of the form (2).

Dynamic regret bounds. The (universal) dynamic regret in OCO compares the learner’s choices with any time-varying comparators, thus serving as a suitable performance measure in non-stationary environments. The path length P_T , introduced by Herbster and Warmuth [18], is a common quantity representing the regularity of the comparator sequence. Zhang et al. [34] achieved the optimal dynamic regret by showing upper and lower bounds with a rate of $\sqrt{T}(1 + P_T)$. Subsequent studies further refined the bound by using data-dependent quantities, including the cumulative loss F_T and the gradient variation [35, 36]. Regarding the connection to online classification, Van der Hoeven et al. [32] mentioned the idea of combining their method with OCO algorithms that enjoy dynamic regret bounds. However, this mention was only made as one example of how their proposed method can be potentially combined with various OCO algorithms, and no resulting bounds on the cumulative target loss were explicitly provided.

2 Preliminaries

For $d \in \mathbb{Z}_{>0}$, let $[d] = \{1, \dots, d\}$. Let $\Delta^d = \{\boldsymbol{\mu} \in \mathbb{R}_{\geq 0}^d : \|\boldsymbol{\mu}\|_1 = 1\}$ denote the probability simplex in \mathbb{R}^d . Let $\|\mathbf{W}\|_{\text{F}} = \sqrt{\text{tr}(\mathbf{W}^\top \mathbf{W})}$ denote the Frobenius norm for any matrix \mathbf{W} . For $\Omega: \mathbb{R}^d \rightarrow \mathbb{R} \cup \{+\infty\}$, let $\Omega^*(\boldsymbol{\theta}) = \sup\{\langle \boldsymbol{\theta}, \boldsymbol{\mu} \rangle - \Omega(\boldsymbol{\mu}) : \boldsymbol{\mu} \in \mathbb{R}^d\}$ be its convex conjugate and let $\text{dom}(\Omega) = \{\boldsymbol{\mu} \in \mathbb{R}^d : \Omega(\boldsymbol{\mu}) < +\infty\}$.

2.1 Problem Setting

We describe details of our problem setting. Examples of problems that fall into our setting include multi-class/multilabel classification and label ranking, which we detail in Appendices A and B. More examples can be found in Blondel [5, Appendix A] and Sakaue et al. [28, Section 2.3 and Appendix C].

Structured prediction. Let $\mathcal{Y} = [K]$ and $\hat{\mathcal{Y}} = [N]$ represent finite sets of labels and predictions, respectively. The set sizes, K and N , can be extremely large when the sets consist of structured objects. A target loss $\ell: \hat{\mathcal{Y}} \times \mathcal{Y} \rightarrow \mathbb{R}_{\geq 0}$ measures the discrepancy between a prediction $\hat{y} \in \hat{\mathcal{Y}}$ and a ground-truth label $y \in \mathcal{Y}$. We can equivalently rewrite $\ell(\hat{y}, y)$ as $\langle \mathbf{e}^y, \ell(\hat{y}) \rangle$, where \mathbf{e}^y is the y th standard basis vector of \mathbb{R}^K and $\ell(\hat{y}) \in \mathbb{R}^K$ is the loss vector whose y th component is $\ell(\hat{y}, y)$ for $y \in \mathcal{Y}$. While this representation applies to any target losses, the vector size K may be very large. Fortunately, more efficient lower-dimensional representations are available for many target losses. As a unifying framework of such target-loss representations, we adopt the following $(\boldsymbol{\rho}, \boldsymbol{\ell}^\boldsymbol{\rho})$ -decomposition of Cao et al. [10].

Definition 2.1. The $(\boldsymbol{\rho}, \boldsymbol{\ell}^\boldsymbol{\rho})$ -decomposition of a target loss $\ell: \hat{\mathcal{Y}} \times \mathcal{Y} \rightarrow \mathbb{R}_{\geq 0}$ is given as follows:

$$\ell(\hat{y}, y) = \langle \boldsymbol{\rho}(y), \boldsymbol{\ell}^\boldsymbol{\rho}(\hat{y}) \rangle + c(y), \quad (3)$$

where $\boldsymbol{\rho}: \mathcal{Y} \rightarrow \mathbb{R}^d$ is a label encoding function into the d -dimensional Euclidean space, $\boldsymbol{\ell}^\boldsymbol{\rho}: \hat{\mathcal{Y}} \rightarrow \mathbb{R}^d$ is the corresponding loss encoding function, and $c: \mathcal{Y} \rightarrow \mathbb{R}$ is the term independent of prediction \hat{y} . We also define $\mathcal{L}^\boldsymbol{\rho} \in \mathbb{R}^{d \times N}$ as the matrix whose column corresponding to $\hat{y} \in \hat{\mathcal{Y}}$ is given by $\boldsymbol{\ell}^\boldsymbol{\rho}(\hat{y})$.

For example, in multiclass classification with $K = d$ classes, we let $\boldsymbol{\rho}(y) = \mathbf{e}^y$, $\boldsymbol{\ell}^\boldsymbol{\rho}(\hat{y}) = \mathbf{1} - \mathbf{e}^{\hat{y}}$, where $\mathbf{1}$ is the all-ones vector, and $c \equiv 0$ to represent the 0-1 target loss. In multilabel classification, a label consists of d binary outcomes, hence $K = 2^d$. Still, the standard Hamming loss enjoys a $(\boldsymbol{\rho}, \boldsymbol{\ell}^\boldsymbol{\rho})$ -decomposition with the dimensionality of $d = \log_2 K$; see Appendix A for details. Throughout this paper, we suppose that the target loss is represented as in (3) with some $\boldsymbol{\rho}$, $\boldsymbol{\ell}^\boldsymbol{\rho}$, and c . Note that this entails no loss of generality since $\boldsymbol{\rho}(y) = \mathbf{e}^y$, $\boldsymbol{\ell}^\boldsymbol{\rho}(\hat{y}) = \ell(\hat{y})$, and $c \equiv 0$ always provide a valid (but possibly inefficient) $(\boldsymbol{\rho}, \boldsymbol{\ell}^\boldsymbol{\rho})$ -decomposition with $d = K$.

Online learning protocol. Let \mathcal{X} be the space of input vectors. For $t = 1, \dots, T$, the environment picks an input $\mathbf{x}_t \in \mathcal{X}$ and ground-truth $y_t \in \mathcal{Y}$. The learner observes \mathbf{x}_t , makes a prediction $\hat{y}_t \in \hat{\mathcal{Y}}$, and observes feedback y_t . The quality of the prediction is measured by the target loss $\ell(\hat{y}_t, y_t)$. The learner's goal is to minimize the cumulative target loss, $\sum_{t=1}^T \ell(\hat{y}_t, y_t)$, over T rounds. The environment may select (\mathbf{x}_t, y_t) adversarially depending on information from rounds $1, \dots, t-1$.

Surrogate loss framework. The surrogate loss framework consists of the space of score vectors \mathbb{R}^d , a surrogate loss function $L: \mathbb{R}^d \times \mathcal{Y} \rightarrow \mathbb{R}_{\geq 0}$, which is convex in the first argument, and a decoding function that converts score vector $\boldsymbol{\theta} \in \mathbb{R}^d$ into prediction $\hat{y} \in \hat{\mathcal{Y}}$. The score space, \mathbb{R}^d , is identical to the output space of the loss encoding function $\boldsymbol{\ell}^\boldsymbol{\rho}$. For convenience, let $\boldsymbol{\pi}: \mathbb{R}^d \rightarrow \Delta^N$ denote a decoding *distribution*, where Δ^N is the probability simplex over the prediction set $\hat{\mathcal{Y}}$, allowing for randomized decoding from $\boldsymbol{\theta} \in \mathbb{R}^d$ to $\hat{y} \in \hat{\mathcal{Y}}$. Let \mathcal{W} be a closed convex set of linear estimators. At the t th round, the learner computes $\boldsymbol{\theta}_t = \mathbf{W}_t \mathbf{x}_t$ with the current linear estimator $\mathbf{W}_t \in \mathcal{W}$ and makes a prediction \hat{y}_t via sampling from the decoding distribution $\boldsymbol{\pi}(\boldsymbol{\theta}_t)$. The surrogate loss, $L(\boldsymbol{\theta}_t, y_t)$, quantifies the discrepancy between the estimated score vector $\boldsymbol{\theta}_t = \mathbf{W}_t \mathbf{x}_t$ and the ground-truth label $y_t \in \mathcal{Y}$. For brevity, let $L_t: \mathcal{W} \mapsto L(\mathbf{W} \mathbf{x}_t, y_t)$ denote the surrogate loss of $\mathbf{W} \in \mathcal{W}$ at round t , which is convex due to the convexity of $\boldsymbol{\theta} \mapsto L(\boldsymbol{\theta}, y)$. Thus, the learner can use OCO algorithms to learn \mathbf{W}_t for $t = 1, \dots, T$.

Assumptions. Below is a list of basic assumptions we make throughout this paper.

Assumption 2.2. *The following conditions hold:*

1. **Target loss can take zero.** $\min_{\hat{y} \in \hat{\mathcal{Y}}} \ell(\hat{y}, y) = 0$ for any ground-truth $y \in \mathcal{Y}$.
2. **Bounded input vectors.** $\|\mathbf{x}_t\|_2 \leq 1$ for $t \in [T]$.
3. **Bounded domain.** There exists $D > 0$ such that $\|\mathbf{W} - \mathbf{W}'\|_{\text{F}} \leq D$ for every $\mathbf{W}, \mathbf{W}' \in \mathcal{W}$.

The first condition holds without loss of generality by adjusting $c(y)$ in Definition 2.1. The second and third bounds are for simplicity. It should, however, be noted that some existing methods can adapt to unknown domain sizes [31, 28].

2.2 Fenchel–Young Loss

The *Fenchel–Young loss* framework [7] offers a convenient recipe for designing various surrogate losses through regularization functions.

Definition 2.3. Let $\Omega: \mathbb{R}^d \rightarrow \mathbb{R} \cup \{+\infty\}$ be a function with $\text{dom}(\Omega) \supseteq \text{conv}(\{\boldsymbol{\rho}(y) \in \mathbb{R}^d : y \in \mathcal{Y}\})$. The Fenchel–Young loss $L_\Omega: \text{dom}(\Omega^*) \times \mathcal{Y} \rightarrow \mathbb{R}_{\geq 0}$ generated by Ω is defined as follows:

$$L_\Omega(\boldsymbol{\theta}, y) = \Omega^*(\boldsymbol{\theta}) + \Omega(\boldsymbol{\rho}(y)) - \langle \boldsymbol{\theta}, \boldsymbol{\rho}(y) \rangle.$$

Fenchel–Young losses are convex in $\boldsymbol{\theta}$, non-negative, and take zero if and only if $\boldsymbol{\rho}(y) \in \partial\Omega^*(\boldsymbol{\theta})$ [7, Proposition 2]. Examples of Fenchel–Young losses include the logistic loss, CRF loss [21], and SparseMAP loss [22]; see Blondel et al. [7, Table 1] for more examples. These surrogate losses are generated by strongly convex regularizers Ω , ensuring that the loss functions are smooth [19, Theorem 6]. The class of surrogate losses we consider is not limited to Fenchel–Young losses of the above form. We can deal with other surrogate losses, such as the smooth hinge loss (see Section 3).

2.3 Dynamic Regret Analysis of OGD

We provide a dynamic regret bound of the online gradient descent (OGD), which we will use to derive our main results. The following guarantee slightly generalizes the original one in Zinkevich [37, Theorem 2] by allowing the learning rate to decrease over time. This might be of independent interest, as existing proofs are, to the best of our knowledge, restricted to the constant learning rate. See Appendix D for the proof.

Proposition 2.4. *Compute $\mathbf{W}_1, \dots, \mathbf{W}_T \in \mathcal{W}$ by applying OGD with non-increasing learning rate $\eta_t > 0$ to convex loss functions $L_t: \mathcal{W} \rightarrow \mathbb{R}$ for $t = 1, \dots, T$; i.e., set \mathbf{W}_1 to an arbitrary point in \mathcal{W} and let*

$$\mathbf{W}_{t+1} = \arg \min \{ \|\mathbf{W}_t - \eta_t \mathbf{G}_t - \mathbf{W}\|_{\text{F}} : \mathbf{W} \in \mathcal{W} \}$$

for $t = 1, \dots, T$, where $\mathbf{G}_t \in \partial L_t(\mathbf{W}_t)$. If the diameter of \mathcal{W} is at most D as in Assumption 2.2, then, for any $\mathbf{U}_1, \dots, \mathbf{U}_T \in \mathcal{W}$ and $P_T = \sum_{t=2}^T \|\mathbf{U}_t - \mathbf{U}_{t-1}\|_{\text{F}}$, we have

$$\sum_{t=1}^T (L_t(\mathbf{W}_t) - L_t(\mathbf{U}_t)) \leq \frac{D}{\eta_T} \left(\frac{D}{2} + P_T \right) + \sum_{t=1}^T \frac{\eta_t}{2} \|\mathbf{G}_t\|_{\text{F}}^2.$$

If \mathbf{U}_t are fixed to the best offline \mathbf{U} , then setting $\eta_t \simeq 1/\sqrt{T}$ for $t \in [T]$ recovers the well-known $O(\sqrt{T})$ regret bound of OGD (regarding D and $\|\mathbf{G}_t\|_{\text{F}}$ as constants).

3 “Small-Surrogate-Loss + Path-Length” Bound via Surrogate Gap

This section considers the setting of prior work [31, 32, 28] and describes our main strategy for the non-stationary setting. Previous studies obtained finite surrogate regret bounds in (1) with a powerful technique known as *exploiting the surrogate gap*. To leverage this, we further restrict the class of target losses from Definition 2.1, which was also assumed in the literature.

Assumption 3.1. *The prediction set equals the label set, i.e., $\hat{\mathcal{Y}} = \mathcal{Y}$. In addition, there exist $\mathbf{V} \in \mathbb{R}^{d \times d}$, $\mathbf{b} \in \mathbb{R}^d$, and $\gamma, \nu > 0$ such that the following conditions hold for some norm $\|\cdot\|$:*

1. $\ell(\hat{y}, y) = \langle \boldsymbol{\rho}(\hat{y}), \mathbf{V}\boldsymbol{\rho}(y) + \mathbf{b} \rangle + c(y)$ for any $y \in \mathcal{Y}$ and $\hat{y} \in \hat{\mathcal{Y}}$,
2. $\mathbb{E}_{\hat{y} \sim \boldsymbol{\pi}}[\ell(\hat{y}, y)] \leq \gamma \|\mathbb{E}_{\hat{y} \sim \boldsymbol{\pi}}[\boldsymbol{\rho}(\hat{y})] - \boldsymbol{\rho}(y)\|$ for any $\boldsymbol{\pi} \in \Delta^N$ and $y \in \mathcal{Y}$, and
3. $\|\boldsymbol{\rho}(y) - \boldsymbol{\rho}(y')\| \geq \nu$ for any $y, y' \in \mathcal{Y}$ with $y \neq y'$.

The first condition means that the target loss is affine decomposable [5, Section 5]. The second one requires that the expected target loss over a distribution $\boldsymbol{\pi}$ is small when the mean prediction is close to ground-truth y . The third one means that distinct labels have distant encodings. These have played essential roles in exploiting the surrogate gap in the previous studies. Examples satisfying these conditions include multiclass and multilabel classification (see Appendix A), and more examples are given in Sakaue et al. [28, Section 2.3 and Appendix C]. Section 4 addresses more general problems that may not satisfy Assumption 3.1. For example, the label ranking problem (see Appendix A.3 for details) does not satisfy $\hat{\mathcal{Y}} = \mathcal{Y}$, which is essential for the remaining three conditions.

3.1 Decoding Methods with Surrogate Gaps

The key to exploiting the surrogate gap lies in decoding, or how to convert a score vector, $\boldsymbol{\theta} = \mathbf{W}\mathbf{x}$, into a prediction $\hat{y} \in \hat{\mathcal{Y}}$. By using existing randomized decoding methods, we can ensure that the expected target loss of \hat{y} is strictly smaller than the surrogate loss of $\boldsymbol{\theta}$. Formally, these methods enable us to sample \hat{y} from a distribution $\boldsymbol{\pi}(\boldsymbol{\theta})$ over $\hat{\mathcal{Y}}$ with the following guarantee.

Assumption 3.2 (Surrogate gap condition). *Let $\ell: \hat{\mathcal{Y}} \times \mathcal{Y} \rightarrow \mathbb{R}_{\geq 0}$ be a target loss, $L: \mathbb{R}^d \times \mathcal{Y} \rightarrow \mathbb{R}_{\geq 0}$ a surrogate loss, and $\alpha \in (0, 1)$. Given any score vector $\boldsymbol{\theta} \in \mathbb{R}^d$, we can draw $\hat{y} \in \hat{\mathcal{Y}}$ following a distribution $\boldsymbol{\pi}(\boldsymbol{\theta}) \in \Delta^N$ that satisfies*

$$\mathbb{E}_{\hat{y} \sim \boldsymbol{\pi}(\boldsymbol{\theta})}[\ell(\hat{y}, y)] \leq (1 - \alpha)L(\boldsymbol{\theta}, y) \quad \text{for any } y \in \mathcal{Y}.$$

That is, the expected target loss, $\mathbb{E}_{\hat{y} \sim \boldsymbol{\pi}(\boldsymbol{\theta})}[\ell(\hat{y}, y)]$, is bounded from above by the surrogate loss, $L(\boldsymbol{\theta}, y)$, subtracted by $\alpha L(\boldsymbol{\theta}, y)$. The last negative term, called the *surrogate gap*, has played a central role in deriving finite surrogate regret bounds in the previous studies. Below are examples of the existing decoding methods:

- For K -class classification with the 0-1 target loss $\ell(\hat{y}, y) = \mathbf{1}_{\hat{y} \neq y}$, which takes one if $\hat{y} \neq y$ and zero otherwise, if L is the smooth hinge loss or logistic loss, randomized decoding methods of Van der Hoeven [31] and Van der Hoeven et al. [32] satisfy Assumption 3.2 with $\alpha = 1/K$.
- For structured prediction problems with Assumption 3.1, if L is a Fenchel–Young loss generated by Ω that is λ -strongly convex ($\lambda > \frac{4\gamma}{\nu}$) with respect to the norm $\|\cdot\|$ introduced in Assumption 3.1,⁴ then the randomized decoding method of Sakaue et al. [28] satisfies Assumption 3.2 with $\alpha = \frac{4\gamma}{\lambda\nu}$.

Note that our analysis below holds as long as Assumption 3.2 is satisfied, while Assumption 3.1 serves merely as a sufficient condition ensuring the availability of decoding methods that satisfy Assumption 3.2.

3.2 Self-Bounding Surrogate Losses

We also introduce the following *self-bounding* property of surrogate losses.

Assumption 3.3 (Self-bounding property). *Let $L_t: \mathcal{W} \ni \mathbf{W} \mapsto L(\mathbf{W}\mathbf{x}_t, y_t)$ be the surrogate loss at round $t \in [T]$. There exists $M > 0$ such that, for every $t \in [T]$ and $\mathbf{W} \in \mathcal{W}$, we can take a subgradient $\mathbf{G}_t(\mathbf{W}) \in \partial L_t(\mathbf{W})$ with $\|\mathbf{G}_t(\mathbf{W})\|_{\mathbf{F}}^2 \leq 2ML_t(\mathbf{W})$.*

⁴In Sakaue et al. [28], Ω is additionally assumed to be of Legendre-type to ensure the self-bounding property. However, it can be obtained only from the strong convexity of Ω [6, Proposition 3].

This property was also assumed in the line of prior work; in particular, Van der Hoeven et al. [32] extensively discussed it.⁵ The property holds for every non-negative M -smooth surrogate loss [23, Theorem 4.23]; hence, Fenchel–Young losses generated by $\frac{1}{M}$ -strongly convex Ω satisfy it. Moreover, it holds for a broader class of losses beyond smooth ones. For example, the smooth hinge loss, viewed as a function of $\mathbf{W} \in \mathcal{W}$, is non-smooth (despite its name); still, it enjoys the self-bounding property, as detailed in Appendix B.1.⁶

3.3 Main Result

We present our main result based on the surrogate gap. The following bound has a significant advantage in non-stationary settings compared to the existing finite surrogate regret bounds (1), yet its proof is simple once we have shown Proposition 2.4, while not obvious a priori.

Theorem 3.4. *Let $\alpha \in (0, 1)$ be the surrogate-gap parameter given in Assumption 3.2 and $M > 0$ the self-bounding parameter given in Assumption 3.3. For $t = 1, \dots, T$, compute $\mathbf{W}_t \in \mathcal{W}$ by using OGD with non-increasing learning rate η_t such that*

$$\frac{\alpha}{M} \leq \eta_t \leq \frac{2(L_t(\mathbf{W}_t) - \mathbb{E}_{\hat{y}_t \sim \pi(\theta_t)}[\ell(\hat{y}_t, y_t)])}{\|\mathbf{G}_t\|_F^2}, \quad (4)$$

where $\pi: \mathbb{R}^d \rightarrow \Delta^N$ is a decoding distribution that satisfies Assumption 3.2 and $\theta_t = \mathbf{W}_t \mathbf{x}_t$. This range of η_t is non-empty, and, for any $\mathbf{U}_1, \dots, \mathbf{U}_T \in \mathcal{W}$, $P_T = \sum_{t=2}^T \|\mathbf{U}_t - \mathbf{U}_{t-1}\|_F$, and $F_T = \sum_{t=1}^T L_t(\mathbf{U}_t)$, we have

$$\sum_{t=1}^T \mathbb{E}_{\hat{y}_t \sim \pi(\theta_t)}[\ell(\hat{y}_t, y_t)] \leq F_T + \frac{MD}{\alpha} \left(\frac{D}{2} + P_T \right).$$

Proof. First, we confirm that the range of η_t in (4) is non-empty. From Assumptions 3.2 and 3.3, we have $L_t(\mathbf{W}_t) - \mathbb{E}_{\hat{y}_t \sim \pi(\theta_t)}[\ell(\hat{y}_t, y_t)] \geq \alpha L_t(\mathbf{W}_t) \geq \frac{\alpha}{2M} \|\mathbf{G}_t\|_F^2$. Thus, $\eta_t = \frac{\alpha}{M}$ always satisfies (4) (regarding the upper bound as $+\infty$ if $\|\mathbf{G}_t\|_F = 0$). To prove the main claim, we use Proposition 2.4 with $\eta_T \geq \frac{\alpha}{M}$ and (4) to obtain

$$\sum_{t=1}^T L_t(\mathbf{W}_t) - \sum_{t=1}^T L_t(\mathbf{U}_t) \leq \frac{MD}{\alpha} \left(\frac{D}{2} + P_T \right) + \sum_{t=1}^T \left(L_t(\mathbf{W}_t) - \mathbb{E}_{\hat{y}_t \sim \pi(\theta_t)}[\ell(\hat{y}_t, y_t)] \right).$$

Rearranging terms yields $\sum_{t=1}^T \mathbb{E}_{\hat{y}_t \sim \pi(\theta_t)}[\ell(\hat{y}_t, y_t)] \leq F_T + \frac{MD}{\alpha} \left(\frac{D}{2} + P_T \right)$, as desired. \square

As discussed in Section 1, if the sequence $(\mathbf{x}_t, y_t)_{t=1}^T$ consists of $O(1)$ intervals of separable data, we can achieve $F_T = 0$ and $P_T = O(1)$ in Theorem 3.4 by changing \mathbf{U}_t $O(1)$ times. This leads to an $O(1)$ bound on the cumulative target loss in this non-stationary setting, while the existing surrogate-regret bound in (1) breaks down.

The essence of the above proof lies in the design of the learning rate η_t in (4). Specifically, the right-hand inequality in (4) enables us to cancel the cumulative surrogate loss terms, $\sum_{t=1}^T L_t(\mathbf{W}_t)$, and to derive an upper bound on the cumulative target loss. Meanwhile, the surrogate-gap condition and the self-bounding property (Assumptions 3.2 and 3.3) guarantee the existence of the lower bound $\eta_T \geq \frac{\alpha}{M}$, which prevents the $O((1 + P_T)/\eta_T)$ term in the OGD regret bound from becoming excessively large. This proof strategy not only extends the original idea of Van der Hoeven [31] to the non-stationary setting, but also offers a more direct derivation of the target-loss bound through learning-rate adjustment in OGD. In the next section, we further discuss how to choose a learning rate η_t that satisfies (4).

As a side note, in the last part of the proof, the bound over the entire interval $t = 1, \dots, T$, is derived simply by summing over $t = 1, \dots, T$. Therefore, the same argument applies to any contiguous subinterval of $1, \dots, T$, with P_T and F_T defined with respect to that subinterval. In this sense, our method enjoys the *strong adaptivity* [15], which is also a desirable property in non-stationary online learning.

⁵Van der Hoeven et al. [32] call self-bounding surrogate losses with an additional property *regular* surrogate losses. The terminology of "self-bounding" follows, e.g., Srebro et al. [30] and Zhao et al. [36].

⁶In Van der Hoeven et al. [32, Appendix A], the hinge loss is also introduced as a self-bounding surrogate loss. However, their hinge loss is discontinuous and hence non-convex. We discuss this point in detail in Appendix C.

3.4 Polyak-Style Learning Rate

The proof of Theorem 3.4 implies that, in theory, setting η_t to the constant, $\frac{\alpha}{M}$, is sufficient. This constant learning rate was employed by Van der Hoeven [31] and Sakaue et al. [28] (whereas Van der Hoeven et al. [32] employed OCO methods with AdaGrad-type regret bounds). In practice, however, $\eta_t = \frac{\alpha}{M}$ would be too conservative, resulting in slow adaptation to dynamic environments. Therefore, we suggest a more adaptive non-increasing learning rate satisfying (4):

$$\eta_t = \min \left\{ \frac{2(L_t(\mathbf{W}_t) - \mathbb{E}_{\hat{y}_t \sim \pi(\boldsymbol{\theta}_t)}[\ell(\hat{y}_t, y_t)])}{\|\mathbf{G}_t\|_F^2}, \eta_{t-1} \right\}, \quad (5)$$

where $\eta_0 = +\infty$ (if $\|\mathbf{G}_t\|_F = 0$, we regard $\eta_t \mathbf{G}_t$ as the zero matrix and make no update). Interestingly, this learning rate is analogous to Polyak's learning rate [24], $\frac{L_t(\mathbf{W}_t) - \min_{\mathbf{W} \in \mathcal{W}} L_t(\mathbf{W})}{\|\mathbf{G}_t\|_F^2}$, which is designed to minimize an upper bound on the suboptimality with respect to L_t . In our setting, the goal is to bound the expected target loss. This motivates replacing $\min_{\mathbf{W} \in \mathcal{W}} L_t(\mathbf{W})$ with $\mathbb{E}_{\hat{y}_t \sim \pi(\boldsymbol{\theta}_t)}[\ell(\hat{y}_t, y_t)]$ (with an adjustment by a factor of two), as in (5). The minimum with η_{t-1} is for ensuring the non-increasing property. In Appendix E, we provide empirical evidence supporting the effectiveness of this Polyak-style learning rate; it matches or outperforms both the constant learning rate $\eta_t = \frac{\alpha}{M}$ and the AdaGrad-type learning rate, with its advantage growing as non-stationarity increases.

When computing the Polyak-style learning rate, we need to evaluate $\mathbb{E}_{\hat{y}_t \sim \pi(\boldsymbol{\theta}_t)}[\ell(\hat{y}_t, y_t)]$, which requires taking the expectation over $\pi(\boldsymbol{\theta}_t) \in \Delta^N$. This can be computed efficiently even in structured prediction settings, where $N = |\hat{\mathcal{Y}}|$ can be exponential in d . Specifically, the randomized decoding of Sakaue et al. [28] obtains $\pi(\boldsymbol{\theta}_t)$ via Frank–Wolfe-type algorithms (e.g., [20]) executed over $\text{conv}(\{\boldsymbol{\rho}(\hat{y}) \in \mathbb{R}^d : \hat{y} \in \hat{\mathcal{Y}}\})$. Such algorithms, combined with techniques for controlling the active-set size [3, 4], return $\pi(\boldsymbol{\theta}_t)$ with the support size of $O(d)$, as guaranteed by Carathéodory's theorem. Thus, we can explicitly compute $\mathbb{E}_{\hat{y}_t \sim \pi(\boldsymbol{\theta}_t)}[\ell(\hat{y}_t, y_t)]$ in polynomial time in d . The same idea works with the decoding method for the convolutional Fenchel–Young loss, discussed in the next section.

4 Addressing More General Problems

This section addresses more general problems that may not satisfy the additional conditions in Assumption 3.1. In fact, many important problems, including label ranking with the normalized discounted cumulative gain (NDCG) loss (see Appendix A.3 for details) and precision at k [5, Appendix A], do not satisfy $\hat{\mathcal{Y}} = \mathcal{Y}$, which is essential for satisfying the conditions in Assumption 3.1. We tackle such problems by leveraging the convolutional Fenchel–Young loss framework.

4.1 Convolutional Fenchel–Young Loss

The convolutional Fenchel–Young loss, proposed by Cao et al. [10], provides an appealing framework for designing smooth surrogate losses that reflect structures of target losses and label sets. Below is the definition.

Definition 4.1 (Convolutional Fenchel–Young Loss). Given a $(\boldsymbol{\rho}, \ell^\boldsymbol{\rho})$ -decomposition of the target loss ℓ in Definition 2.1, define $\tau: \mathbb{R}^d \rightarrow \mathbb{R}$ as follows.⁷

$$\tau(\boldsymbol{\mu}) = -\min \left\{ \langle \boldsymbol{\mu}, \ell^\boldsymbol{\rho}(\hat{y}) \rangle : \hat{y} \in \hat{\mathcal{Y}} \right\}.$$

Then, the convolutional Fenchel–Young loss $L_{\Omega_\tau}: \mathbb{R}^d \times \mathcal{Y} \rightarrow \mathbb{R}_{\geq 0}$ is defined as follows:

$$L_{\Omega_\tau}(\boldsymbol{\theta}, y) = \Omega_\tau^*(\boldsymbol{\theta}) + \Omega_\tau(\boldsymbol{\rho}(y)) - \langle \boldsymbol{\theta}, \boldsymbol{\rho}(y) \rangle,$$

where $\Omega_\tau(\boldsymbol{\mu}) = \Omega(\boldsymbol{\mu}) + \tau(\boldsymbol{\mu})$ for any $\boldsymbol{\mu} \in \mathbb{R}^d$ and $\Omega: \mathbb{R}^d \rightarrow \mathbb{R} \cup \{+\infty\}$ is a regularization function.

⁷This represents the negative of the Bayes risk of ℓ at $\boldsymbol{\eta} \in \Delta^K$ with $\boldsymbol{\mu} = \mathbb{E}_{y \sim \boldsymbol{\eta}}[\boldsymbol{\rho}(y)]$, shifted by $\mathbb{E}_{y \sim \boldsymbol{\eta}}[c(y)]$.

A convolutional Fenchel–Young loss is merely a specific instance of Fenchel–Young losses with regularizer Ω_τ . Nevertheless, this particular design of the Fenchel–Young loss is noteworthy for statistical learning because, by using strongly convex Ω , we can construct a smooth surrogate loss whose excess risk linearly upper bounds the target excess risk [10, Theorem 15].

Below, let $\mathcal{C} = \text{conv}(\{\boldsymbol{\rho}(y) \in \mathbb{R}^d : y \in \mathcal{Y}\})$ and assume that Ω in Definition 4.1 satisfies the condition below.⁸

Assumption 4.2. *The function Ω in Definition 4.1 satisfies $\text{dom}(\Omega) = \mathcal{C}$ and is λ -strongly convex over \mathcal{C} with respect to the ℓ_2 -norm for some $\lambda > 0$.*

This is a mild requirement. We can always satisfy it by defining Ω as the sum of λ -strongly convex function Ψ with $\mathcal{C} \subseteq \text{dom}(\Psi)$ and the indicator function of \mathcal{C} . An example of convolutional Fenchel–Young losses with Ω being the negative Shannon entropy is given in Cao et al. [10, Section 4]. Also, Appendix B.3 discusses an example for label ranking with the NDCG target loss (see also Appendix A.3). Blondel et al. [7, Section 3.2] also discuss regularizers satisfying Assumption 4.2.

4.2 Key Lemmas

While the convolutional Fenchel–Young loss has been thoroughly investigated by Cao et al. [10] from the perspective of statistical learning, applying it to our online learning setting requires new technical tools. The proofs of the following lemmas are given in Appendix F.

One such tool is the following target–surrogate relationship, which serves as an alternative to the surrogate-gap condition (Assumption 3.2) in Section 3. While this is a newly established relationship, it is related to Cao et al. [10, Theorem 15]; see Appendix F.2 for details.

Lemma 4.3 (Target–surrogate relation). *Let $(\boldsymbol{\theta}, y) \in \mathbb{R}^d \times \mathcal{Y}$ and define a decoding distribution as*

$$\boldsymbol{\pi}(\boldsymbol{\theta}) \in \arg \min_{\boldsymbol{\pi} \in \Delta^N} \Omega^*(\boldsymbol{\theta} + \mathcal{L}^\rho \boldsymbol{\pi}). \quad (6)$$

Draw \hat{y} from $\hat{\mathcal{Y}}$ following $\boldsymbol{\pi}(\boldsymbol{\theta}) \in \Delta^N$. Then, we have

$$\mathbb{E}_{\hat{y} \sim \boldsymbol{\pi}(\boldsymbol{\theta})}[\ell(\hat{y}, y)] = L_{\Omega_\tau}(\boldsymbol{\theta}, y) - L_\Omega(\boldsymbol{\theta} + \mathcal{L}^\rho \boldsymbol{\pi}(\boldsymbol{\theta}), y). \quad (7)$$

The distribution $\boldsymbol{\pi}(\boldsymbol{\theta})$ in (6) can be computed efficiently in most cases, with the support size being polynomial in d ; see Cao et al. [10, Section 4] and Appendix B.3.

Additionally, the following lower bound on $L_\Omega(\boldsymbol{\theta} + \mathcal{L}^\rho \boldsymbol{\pi}(\boldsymbol{\theta}), y)$, the negative term in (7), serves as an alternative to the self-bounding property (Assumption 3.3).

Lemma 4.4. *Under Assumption 4.2 and the same conditions as Lemma 4.3, it holds that*

$$L_\Omega(\boldsymbol{\theta} + \mathcal{L}^\rho \boldsymbol{\pi}(\boldsymbol{\theta}), y) \geq \frac{\lambda}{2} \|\nabla L_{\Omega_\tau}(\boldsymbol{\theta}, y)\|_2^2.$$

4.3 Main Result

Now we are ready to prove our main result, a “small-surrogate-loss + path-length” bound for the broader class of problems that may not satisfy Assumption 3.1. The following theorem is obtained by applying the same OGD as that in Theorem 3.4 to the convolutional Fenchel–Young loss. Thus, we can use the Polyak-style learning rate discussed in Section 3.4.

Theorem 4.5. *Let $L_t: \mathbf{W} \mapsto L_{\Omega_\tau}(\mathbf{W} \mathbf{x}_t, y_t)$ be a convolutional Fenchel–Young loss, where $\Omega_\tau = \Omega + \tau$ and Ω satisfies Assumption 4.2. For $t = 1, \dots, T$, compute $\mathbf{W}_t \in \mathcal{W}$ by using OGD with non-increasing learning rate η_t such that*

$$\lambda \leq \eta_t \leq \frac{2(L_t(\mathbf{W}_t) - \mathbb{E}_{\hat{y}_t \sim \boldsymbol{\pi}(\boldsymbol{\theta}_t)}[\ell(\hat{y}_t, y_t)])}{\|\mathbf{G}_t\|_{\text{F}}^2}, \quad (8)$$

⁸Under Assumption 4.2, Ω is closed proper convex and $\text{dom}(\Omega)$ is bounded. Consequently, Ω is *co-finite* and hence $\text{dom}(\Omega^*) = \mathbb{R}^d$ [26, Corollary 13.3.1]. These guarantee that Cao et al. [10, Condition 1] holds.

where $\boldsymbol{\theta}_t = \mathbf{W}_t \mathbf{x}_t$ and $\boldsymbol{\pi}(\boldsymbol{\theta}_t) \in \arg \min_{\boldsymbol{\pi} \in \Delta^N} \Omega^*(\boldsymbol{\theta}_t + \mathcal{L}^\rho \boldsymbol{\pi})$ is the decoding distribution given in (6). This range of η_t is non-empty and, for any $\mathbf{U}_1, \dots, \mathbf{U}_T \in \mathcal{W}$, $P_T = \sum_{t=2}^T \|\mathbf{U}_t - \mathbf{U}_{t-1}\|_F$, and $F_T = \sum_{t=1}^T L_t(\mathbf{U}_t)$, it holds that

$$\sum_{t=1}^T \mathbb{E}_{\hat{y}_t \sim \boldsymbol{\pi}(\boldsymbol{\theta}_t)} [\ell(\hat{y}_t, y_t)] \leq F_T + \frac{D}{\lambda} \left(\frac{D}{2} + P_T \right).$$

Proof. Again, we begin by confirming that the range of η_t in (8) is non-empty. Lemmas 4.3 and 4.4 imply

$$L_t(\mathbf{W}_t) - \mathbb{E}_{\hat{y}_t \sim \boldsymbol{\pi}(\boldsymbol{\theta}_t)} [\ell(\hat{y}_t, y_t)] = L_\Omega(\boldsymbol{\theta}_t + \mathcal{L}^\rho \boldsymbol{\pi}(\boldsymbol{\theta}_t), y_t) \geq \frac{\lambda}{2} \|\nabla L_{\Omega_\tau}(\boldsymbol{\theta}_t, y_t)\|_2^2,$$

and the right-hand side is bounded below by $\frac{\lambda}{2} \|\mathbf{G}_t\|_F^2$ as $\|\mathbf{G}_t\|_F^2 = \|\nabla L_{\Omega_\tau}(\boldsymbol{\theta}_t, y_t)\|_2^2 \|\mathbf{x}_t\|_2^2 \leq \|\nabla L_{\Omega_\tau}(\boldsymbol{\theta}_t, y_t)\|_2^2$ due to $\|\mathbf{x}_t\|_2 \leq 1$ (Assumption 2.2). Therefore, $\eta_t = \lambda$ always satisfies (8). To prove the main claim, we use Proposition 2.4 with $\eta_T \geq \lambda$ and (8), obtaining

$$\sum_{t=1}^T (L_t(\mathbf{W}_t) - L_t(\mathbf{U}_t)) \leq \frac{D}{\lambda} \left(\frac{D}{2} + P_T \right) + \sum_{t=1}^T (L_t(\mathbf{W}_t) - \mathbb{E}_{\hat{y}_t \sim \boldsymbol{\pi}(\boldsymbol{\theta}_t)} [\ell(\hat{y}_t, y_t)]).$$

Rearranging terms yields $\sum_{t=1}^T \mathbb{E}_{\hat{y}_t \sim \boldsymbol{\pi}(\boldsymbol{\theta}_t)} [\ell(\hat{y}_t, y_t)] \leq F_T + \frac{D}{\lambda} \left(\frac{D}{2} + P_T \right)$, as desired. \square

Let us discuss the difference from the analysis in Theorem 3.4. In that proof, we used the surrogate-gap condition, $L_t(\mathbf{W}_t) - \mathbb{E}_{\hat{y}_t \sim \boldsymbol{\pi}(\boldsymbol{\theta}_t)} [\ell(\hat{y}_t, y_t)] \geq \alpha L_t(\mathbf{W}_t)$, to obtain the desired bound. In the general setting considered here, no decoding method is known that guarantees such a condition. Fortunately, however, Lemmas 4.3 and 4.4 enable us to ensure the alternative condition, $L_t(\mathbf{W}_t) - \mathbb{E}_{\hat{y}_t \sim \boldsymbol{\pi}(\boldsymbol{\theta}_t)} [\ell(\hat{y}_t, y_t)] \geq \frac{\lambda}{2} \|\mathbf{G}_t\|_F^2$. Roughly speaking, this condition is easier to satisfy given $\|\mathbf{G}_t\|_F^2 \leq \frac{2}{\lambda} L_t(\mathbf{W}_t)$, which follows from the self-bounding property of L_t (Assumption 3.3) implied by the λ -strong convexity of Ω_τ . The above proof shows that this weaker requirement is sufficient to derive the “small-surrogate-loss + path-length” bound.

As a cautionary note, one might be tempted to increase the strong convexity parameter λ arbitrarily to shrink the $O((1+P_T)/\lambda)$ term; however, this simultaneously increases the scale of L_{Ω_τ} and thus enlarges F_T (see also [7, Proposition 2]). The value of λ should be chosen to balance this trade-off.

5 Lower Bound

We present a lower bound to complement our upper bounds discussed so far.

Theorem 5.1. *For any possibly randomized learner, there exist an instance of online binary classification with the 0-1 target loss and the smooth hinge surrogate loss such that $\mathbb{E}[\sum_{t=1}^T \ell(\hat{y}_t, y_t)] = \Omega(P_T)$ holds for a sequence $\mathbf{U}_1, \dots, \mathbf{U}_T$ and $\mathbb{E}[\sum_{t=1}^T \ell(\hat{y}_t, y_t)] = \Omega(F_T)$ for another sequence, where the expectation is taken over the learner’s possible randomness. In particular, this means that $\mathbb{E}[\sum_{t=1}^T \ell(\hat{y}_t, y_t)] = O(F_T^{1-\varepsilon_F} + P_T^{1-\varepsilon_P})$ is unattainable for any $\varepsilon_F, \varepsilon_P \geq 0$ with $\varepsilon_F + \varepsilon_P > 0$.*

We provide the proof in Appendix G. This lower bound suggests that the linear dependence on neither F_T nor P_T can be improved in the worst case. Note that our upper bounds apply to any comparators, and hence we may use any comparators to prove the lower bound.

Note that the lower bound might be avoided by focusing on specific instances other than binary classification with the smooth hinge surrogate loss. Theorem 5.1 is intended to complement our upper bounds, which apply to general settings that subsume this specific instance.

6 Conclusion

We have obtained “small-surrogate-loss + path-length” bounds on the cumulative target loss for non-stationary online structured prediction. The core idea is to synthesize the dynamic regret analysis of OGD with the

surrogate gap. En route to this, we have introduced a new Polyak-style learning rate, which automatically offers guarantees on the target loss and works well empirically. Then, we have extended this approach to the broader class of problems than previously considered by leveraging the convolutional Fenchel–Young loss. This has been enabled by new technical lemmas on the convolutional Fenchel–Young loss. Finally, we have obtained a lower bound to complement the upper bounds.

As regards limitations, this work is restricted to full-information feedback. Existing surrogate regret bounds under more limited feedback, such as bandit feedback, explicitly depend on T [31, 32, 29], unlike the full-information case. Thus, obtaining meaningful guarantees by using dynamic regret bounds in such settings poses a new challenge, which is left for future work.

Acknowledgements

SS is supported by JST BOOST Program Grant Number JPMJBY24D1. HB is supported by JST PRESTO Grant Number JPMJPR24K6. YC is supported by Google PhD Fellowship program.

References

- [1] G. BakIr, T. Hofmann, B. Schölkopf, A. J. Smola, B. Taskar, and S. V. N. Vishwanathan. *Predicting Structured Data*. The MIT Press, 2007 (cited on page 1).
- [2] P. L. Bartlett, M. I. Jordan, and J. D. McAuliffe. Convexity, classification, and risk bounds. *Journal of the American Statistical Association*, 101(473):138–156, 2006 (cited on page 1).
- [3] A. Beck and S. Shtern. Linearly convergent away-step conditional gradient for non-strongly convex functions. *Mathematical Programming*, 164:1–27, 2017 (cited on pages 8, 17).
- [4] M. Besançon, S. Pokutta, and E. S. Wirth. The pivoting framework: Frank–Wolfe algorithms with active set size control. In *Proceedings of the 28th International Conference on Artificial Intelligence and Statistics*, volume 258, pages 271–279. PMLR, 2025 (cited on pages 8, 17).
- [5] M. Blondel. Structured prediction with projection oracles. In *Advances in Neural Information Processing Systems*, volume 32, pages 12167–12178. Curran Associates, Inc., 2019 (cited on pages 3, 4, 6, 8, 14).
- [6] M. Blondel, F. Llinares-Lopez, R. Dadashi, L. Hussenot, and M. Geist. Learning energy networks with generalized Fenchel–Young losses. In *Advances in Neural Information Processing Systems*, volume 35, pages 12516–12528. Curran Associates, Inc., 2022 (cited on pages 6, 15, 21).
- [7] M. Blondel, A. F. T. Martins, and V. Niculae. Learning with Fenchel–Young losses. *Journal of Machine Learning Research*, 21(35):1–69, 2020 (cited on pages 3, 5, 9, 10, 15, 16).
- [8] P. Boudart, A. Rudi, and P. Gaillard. Structured prediction in online learning. *arXiv:2406.12366*, 2024 (cited on page 3).
- [9] S. Boyd and L. Vandenberghe. *Convex Optimization*. Cambridge University Press, 2004 (cited on page 15).
- [10] Y. Cao, H. Bao, L. Feng, and B. An. Establishing linear surrogate regret bounds for convex smooth losses via convolutional Fenchel–Young losses. *arXiv:2505.09432*, 2025 (cited on pages 3, 4, 8, 9, 16, 17, 20, 21).
- [11] N. Cesa-Bianchi and G. Lugosi. *Prediction, Learning, and Games*. Cambridge University Press, 2006 (cited on page 2).
- [12] C. Ciliberto, L. Rosasco, and A. Rudi. A consistent regularization approach for structured prediction. In *Advances in Neural Information Processing Systems*, volume 29, pages 4412–4420. Curran Associates, Inc., 2016 (cited on pages 2, 3).
- [13] C. Ciliberto, L. Rosasco, and A. Rudi. A general framework for consistent structured prediction with implicit loss embeddings. *Journal of Machine Learning Research*, 21(98):1–67, 2020 (cited on pages 2, 3).

[14] K. Crammer and Y. Singer. On the algorithmic implementation of multiclass kernel-based vector machines. *Journal of Machine Learning Research*, 2:265–292, 2001 (cited on pages 15, 17).

[15] A. Daniely, A. Gonen, and S. Shalev-Shwartz. Strongly adaptive online learning. In *Proceedings of the 32nd International Conference on Machine Learning*, volume 37, pages 1405–1411. PMLR, 2015 (cited on page 7).

[16] J. M. Danskin. The theory of max-min, with applications. *SIAM Journal on Applied Mathematics*, 14(4):641–664, 1966 (cited on pages 16, 21).

[17] D. Garber and N. Wolf. Frank–Wolfe with a nearest extreme point oracle. In *Proceedings of the 34th Conference on Learning Theory*, volume 134, pages 2103–2132. PMLR, 2021 (cited on page 16).

[18] M. Herbster and M. K. Warmuth. Tracking the best linear predictor. *Journal of Machine Learning Research*, 1:281–309, 2001 (cited on page 3).

[19] S. M. Kakade, S. Shalev-Shwartz, and A. Tewari. On the duality of strong convexity and strong smoothness: Learning applications and matrix regularization. Technical report, 2009 (cited on page 5).

[20] S. Lacoste-Julien and M. Jaggi. On the global linear convergence of Frank–Wolfe optimization variants. In *Advances in Neural Information Processing Systems*, volume 28, pages 496–504. Curran Associates, Inc., 2015 (cited on pages 8, 16).

[21] J. Lafferty, A. McCallum, and F. C. N. Pereira. Conditional random fields: Probabilistic models for segmenting and labeling sequence data. In *Proceedings of the 18th International Conference on Machine Learning*, pages 282–289. Morgan Kaufmann Publishers Inc., 2001 (cited on page 5).

[22] V. Niculae, A. F. T. Martins, M. Blondel, and C. Cardie. SparseMAP: Differentiable sparse structured inference. In *Proceedings of the 35th International Conference on Machine Learning*, volume 80, pages 3799–3808. PMLR, 2018 (cited on pages 5, 16).

[23] F. Orabona. A modern introduction to online learning. *arXiv:1912.13213*, 2023. <https://arxiv.org/abs/1912.13213v6> (cited on pages 2, 7, 18, 19).

[24] B. T. Polyak. *Introduction to Optimization*. Optimization Software, 1987 (cited on page 8).

[25] J. D. M. Rennie and N. Srebro. Loss functions for preference levels: Regression with discrete ordered labels. In *Proceedings of the IJCAI Multidisciplinary Workshop on Advances in Preference Handling*, pages 180–186. Kluwer Norwell, 2005 (cited on page 15).

[26] R. T. Rockafellar. *Convex Analysis*. Princeton University Press, 1970 (cited on page 9).

[27] F. Rosenblatt. The perceptron: A probabilistic model for information storage and organization in the brain. *Psychological Review*, 65(6):386–408, 1958 (cited on pages 2, 3).

[28] S. Sakaue, H. Bao, T. Tsuchiya, and T. Oki. Online structured prediction with Fenchel–Young losses and improved surrogate regret for online multiclass classification with logistic loss. In *Proceedings of the 37th Conference on Learning Theory*, volume 247, pages 4458–4486. PMLR, 2024 (cited on pages 2–6, 8, 14, 16, 19).

[29] Y. Shibukawa, T. Tsuchiya, S. Sakaue, and K. Yamanishi. Bandit and delayed feedback in online structured prediction. *arXiv:2502.18709*, 2025 (cited on pages 2, 3, 11).

[30] N. Srebro, K. Sridharan, and A. Tewari. Smoothness, low noise and fast rates. In *Advances in Neural Information Processing Systems*, volume 23, pages 2199–2207. Curran Associates, Inc., 2010 (cited on page 7).

[31] D. Van der Hoeven. Exploiting the surrogate gap in online multiclass classification. In *Advances in Neural Information Processing Systems*, volume 33, pages 9562–9572. Curran Associates, Inc., 2020 (cited on pages 2, 3, 5–8, 11, 14, 16, 17, 19).

[32] D. Van der Hoeven, F. Fusco, and N. Cesa-Bianchi. Beyond bandit feedback in online multiclass classification. In *Advances in Neural Information Processing Systems*, volume 34, pages 13280–13291. Curran Associates, Inc., 2021 (cited on pages 2, 3, 5–8, 11, 14, 16, 17, 19).

- [33] A. C.-C. Yao. Probabilistic computations: Toward a unified measure of complexity. In *Proceedings of the 18th Annual Symposium on Foundations of Computer Science*, pages 222–227. IEEE, 1977 (cited on page 21).
- [34] L. Zhang, S. Lu, and Z.-H. Zhou. Adaptive online learning in dynamic environments. In *Advances in Neural Information Processing Systems*, volume 31, pages 1323–1333. Curran Associates, Inc., 2018 (cited on page 3).
- [35] P. Zhao, Y.-J. Zhang, L. Zhang, and Z.-H. Zhou. Dynamic regret of convex and smooth functions. In *Advances in Neural Information Processing Systems*, volume 33, pages 12510–12520. Curran Associates, Inc., 2020 (cited on page 3).
- [36] P. Zhao, Y.-J. Zhang, L. Zhang, and Z.-H. Zhou. Adaptivity and non-stationarity: Problem-dependent dynamic regret for online convex optimization. *Journal of Machine Learning Research*, 25(98):1–52, 2024 (cited on pages 2, 3, 7).
- [37] M. Zinkevich. Online convex programming and generalized infinitesimal gradient ascent. In *Proceedings of the 20th International Conference on Machine Learning*, pages 928–935. AAAI Press, 2003 (cited on pages 2, 3, 5).

A Examples of Structured Prediction Problems

Below we discuss a part of examples provided in Blondel [5] and Sakaue et al. [28].

A.1 Multiclass Classification

Let $\mathcal{Y} = \hat{\mathcal{Y}} = [K]$ and $\ell(\hat{y}, y) = \mathbb{1}_{\hat{y} \neq y}$ be the 0-1 loss, which trivially satisfies the zero-loss condition in Assumption 2.2. An affine decomposition of the dimensionality $d = K$ (see Assumption 3.1) is given by $\rho(y) = \mathbf{e}^y$, $\mathbf{V} = \mathbf{1}\mathbf{1}^\top - I$, $\mathbf{b} = 0$, and $c \equiv 0$, where $\mathbf{1} \in \mathbb{R}^d$ is the all-ones vector and $I \in \mathbb{R}^{d \times d}$ is the identity matrix, i.e., $\ell(\hat{y}, y) = \langle \mathbf{e}^{\hat{y}}, (\mathbf{1}\mathbf{1}^\top - I)\mathbf{e}^y \rangle = \langle \mathbf{e}^{\hat{y}}, \mathbf{1} - \mathbf{e}^y \rangle$. Let $\pi \in \Delta^d$ and $\hat{\mu} = \mathbb{E}_{\hat{y} \sim \pi} \mathbf{e}^{\hat{y}} \in \Delta^d$. Then, we have $\mathbb{E}_{\hat{y} \sim \pi} [\ell(\hat{y}, y)] = \langle \hat{\mu}, \mathbf{1} - \mathbf{e}^y \rangle = \frac{1}{2} \|\hat{\mu} - \mathbf{e}^y\|_1$ for any $y \in \mathcal{Y}$ and $\|\mathbf{e}^y - \mathbf{e}^{y'}\|_1 = 2$ for any $y, y' \in \mathcal{Y}$ with $y \neq y'$. Therefore, the conditions in Assumption 3.1 are satisfied.

A.2 Multilabel Classification

Consider predicting d binary outcomes, 0 or 1. Let $\mathcal{Y} = \hat{\mathcal{Y}} = [K]$ for $K = 2^d$. For the target loss, we use the Hamming loss, $\ell(\hat{y}, y) = \frac{1}{d} \sum_{i=1}^d \mathbb{1}_{\hat{y}_i \neq y_i}$, where \hat{y}_i and y_i are the i th outcome of $\hat{y} \in \hat{\mathcal{Y}}$ and $y \in \mathcal{Y}$, respectively, for $i \in [d]$. This target loss trivially satisfies the zero-loss condition in Assumption 2.2. A d -dimensional affine decomposition of the Hamming loss is given as follows: let $\rho(y) \in \{0, 1\}^d$ be a vector whose i th element represents the i th outcome of y , $\mathbf{V} = -\frac{2}{d}I$, $\mathbf{b} = \frac{1}{d}\mathbf{1}$, and $c(y) = \frac{1}{d}\langle \rho(y), \mathbf{1} \rangle$; then, it holds that $\ell(\hat{y}, y) = \frac{1}{d}(\langle \rho(\hat{y}), \mathbf{1} \rangle + \langle \rho(y), \mathbf{1} \rangle - 2\langle \rho(\hat{y}), \rho(y) \rangle)$. We also have $\mathbb{E}_{\hat{y} \sim \pi} [\ell(\hat{y}, y)] = \frac{1}{d} \|\mathbb{E}_{\hat{y} \sim \pi} \rho(\hat{y}) - \rho(y)\|_1$ for any $y \in \mathcal{Y}$ and $\|\rho(y) - \rho(y')\|_1 \geq 1$ for any $y, y' \in \mathcal{Y}$ with $y \neq y'$. Therefore, Assumption 3.1 is satisfied.

A.3 Ranking with NDCG Loss

Consider predicting ranking of documents, a common task in information retrieval. Let $\mathcal{Y} = [k]^d$ be the set of relevance scores of d documents and $\hat{\mathcal{Y}}$ the permutations of $[d]$. The normalized discounted cumulative gain (NDCG) loss $\ell: \hat{\mathcal{Y}} \times \mathcal{Y} \rightarrow \mathbb{R}_{\geq 0}$ with weights $w_1, \dots, w_d \geq 0$ is defined as follows:

$$\ell(\hat{y}, y) = 1 - \frac{1}{N(y)} \sum_{i=1}^d y_i w_{\hat{y}(i)},$$

where $y_i \in [k]$ is the relevance score of the i th document, $\hat{y}(i) \in [d]$ is the i th element of permutation \hat{y} of $[d]$, and $N(y) = \max_{\hat{y} \in \hat{\mathcal{Y}}} \sum_{i=1}^d y_i w_{\hat{y}(i)}$ is the normalization constant. A d -dimensional (ρ, ℓ^ρ) -decomposition of this loss is given by $\rho(y) = -(y_1, \dots, y_d)^\top / N(y)$, $\ell^\rho(\hat{y}) = (w_{\hat{y}(1)}, \dots, w_{\hat{y}(d)})^\top$, and $c \equiv 1$. Setting \hat{y} to the best permutation (a maximizer in the definition of $N(y)$) makes the loss zero. Note that this example does not satisfy the additional assumptions in Assumption 3.1 due to $\mathcal{Y} \neq \hat{\mathcal{Y}}$. Still, the framework in Section 4 can handle this case by using a convolutional Fenchel–Young loss as a surrogate loss.

B Examples of Surrogate Losses

We provide examples of surrogate losses. All of them indeed satisfy the self-bounding property in Assumption 3.3.

B.1 Smooth Hinge Loss

We describe the details of the smooth hinge loss used in Van der Hoeven [31] and Van der Hoeven et al. [32]. For any $\mathbf{W} \in \mathcal{W}$, we define the multiclass margin of \mathbf{W} at round t as follows:

$$m_t(\mathbf{W}, y_t) = \langle \mathbf{e}^{y_t}, \mathbf{W} \mathbf{x}_t \rangle - \max_{y \neq y_t} \langle \mathbf{e}^y, \mathbf{W} \mathbf{x}_t \rangle.$$

The smooth hinge loss of Rennie and Srebro [25] (strictly speaking, its multiclass extension based on [14]) is defined as follows:

$$L_t(\mathbf{W}) = L(\mathbf{W}\mathbf{x}_t, y_t) = \begin{cases} 1 - 2m_t(\mathbf{W}, y_t) & \text{if } m_t(\mathbf{W}, y_t) \leq 0, \\ \max\{1 - m_t(\mathbf{W}, y_t), 0\}^2 & \text{if } m_t(\mathbf{W}, y_t) > 0. \end{cases}$$

We can check the convexity of $L_t(\mathbf{W})$ as follows: $m_t(\mathbf{W}, y_t)$ is concave in \mathbf{W} since it is the negative of the pointwise maximum of linear functions, and $L_t(\mathbf{W})$ viewed as a univariate function of $m_t(\mathbf{W}, y_t)$ is convex and non-increasing; the composition of these two functions is convex [9, Section 3.2.4].

For convenience, we also define

$$m_t^*(\mathbf{W}) = \max_{y \in \mathcal{Y}} m_t(\mathbf{W}, y) \quad \text{and} \quad y_t^* \in \arg \max_{y \in \mathcal{Y}} \langle \mathbf{e}^y, \mathbf{W}\mathbf{x}_t \rangle.$$

Note that, for any $y' \in \mathcal{Y} \setminus \{y_t^*\}$, we have

$$m_t(\mathbf{W}, y') = \langle \mathbf{e}^{y'}, \mathbf{W}\mathbf{x}_t \rangle - \max_{y \neq y'} \langle \mathbf{e}^y, \mathbf{W}\mathbf{x}_t \rangle = \langle \mathbf{e}^{y'}, \mathbf{W}\mathbf{x}_t \rangle - \langle \mathbf{e}^{y_t^*}, \mathbf{W}\mathbf{x}_t \rangle \leq 0.$$

In addition, if $y_t^* = y_t$, we have

$$m_t(\mathbf{W}, y_t) = \langle \mathbf{e}^{y_t^*}, \mathbf{W}\mathbf{x}_t \rangle - \max_{y \neq y_t} \langle \mathbf{e}^y, \mathbf{W}\mathbf{x}_t \rangle \geq 0.$$

Therefore, under $y_t^* = y_t$, we have $m_t^*(\mathbf{W}) = m_t(\mathbf{W}, y_t^*) = m_t(\mathbf{W}, y_t) \geq 0$.

Defining $\tilde{y}_t \in \arg \max_{y \neq y_t} \langle \mathbf{e}^y, \mathbf{W}\mathbf{x}_t \rangle$, we can express a subgradient of L_t at \mathbf{W} as follows:

$$\mathbf{G}_t(\mathbf{W}) = \begin{cases} 2(\mathbf{e}^{\tilde{y}_t} - \mathbf{e}^{y_t})\mathbf{x}_t^\top & \text{if } y_t^* \neq y_t, \\ 2(1 - m_t^*(\mathbf{W}))(\mathbf{e}^{\tilde{y}_t} - \mathbf{e}^{y_t})\mathbf{x}_t^\top & \text{if } y_t^* = y_t \text{ and } m_t^*(\mathbf{W}) < 1, \\ 0 & \text{if } y_t^* = y_t \text{ and } m_t^*(\mathbf{W}) \geq 1, \end{cases}$$

where 0 means the all-zero matrix. Thus, $\|\mathbf{G}_t(\mathbf{W})\|_F \leq 2\sqrt{2}\|\mathbf{x}_t\|_2 \leq 2\sqrt{2}$ holds in any case. As for the self-bounding property, the third case is trivial. In the first case, $y_t^* \neq y_t$ implies $m_t(\mathbf{W}, y_t) \leq 0$ and hence

$$\|\mathbf{G}_t(\mathbf{W})\|_F^2 = 8\|\mathbf{x}_t\|_2^2 \leq 8L_t(\mathbf{W}).$$

In the second case, we have

$$\|\mathbf{G}_t(\mathbf{W})\|_F^2 = 8(1 - m_t^*(\mathbf{W}))^2\|\mathbf{x}_t\|_2^2 \leq 8L_t(\mathbf{W}).$$

Thus, $\|\mathbf{G}_t(\mathbf{W})\|_F^2 \leq 8L_t(\mathbf{W})$ holds in any case. Note that L_t is non-smooth in $\mathbf{W} \in \mathcal{W}$ since, if multiple \tilde{y}_t attain $\max_{y \neq y_t} \langle \mathbf{e}^y, \mathbf{W}\mathbf{x}_t \rangle$, then the subgradients are non-unique, violating the smoothness (or the Lipschitz continuity of the gradient). We remark that this non-smoothness is caused by the multiclass margin $m_t(\mathbf{W}, y_t)$; indeed, L_t viewed as a univariate function of $m_t(\mathbf{W}, y_t)$ is smooth.

B.2 Fenchel–Young Loss

Consider using the Fenchel–Young loss defined in Section 2.2 as a surrogate loss, namely,

$$L_t(\mathbf{W}) = L_\Omega(\mathbf{W}\mathbf{x}_t, y_t) = \Omega^*(\mathbf{W}\mathbf{x}_t) + \Omega(\boldsymbol{\rho}(y_t)) - \langle \mathbf{W}\mathbf{x}_t, \boldsymbol{\rho}(y_t) \rangle.$$

We assume the regularizer Ω to be λ -strongly convex with respect to the Euclidean norm. For convenience, let $\mathcal{C} = \text{conv}(\{\boldsymbol{\rho}(y) \in \mathbb{R}^d : y \in \mathcal{Y}\})$ and $\boldsymbol{\theta} = \mathbf{W}\mathbf{x}_t$. We define the regularized prediction (strictly speaking, its encoded vector) as

$$\boldsymbol{\rho}_\Omega(\boldsymbol{\theta}) = \arg \max\{ \langle \boldsymbol{\theta}, \boldsymbol{\mu} \rangle - \Omega(\boldsymbol{\mu}) : \boldsymbol{\mu} \in \mathcal{C} \}.$$

Then, it holds that $\nabla L_t(\mathbf{W}) = (\boldsymbol{\rho}_\Omega(\boldsymbol{\theta}) - \boldsymbol{\rho}(y_t))\mathbf{x}_t^\top$ [7, Proposition 2], which means that $\|\nabla L_t(\mathbf{W})\|_F$ is at most the ℓ_2 -diameter of \mathcal{C} . Moreover, we have $\frac{\lambda}{2}\|\boldsymbol{\rho}_\Omega(\boldsymbol{\theta}) - \boldsymbol{\rho}(y_t)\|_2^2 \leq L_t(\mathbf{W})$ due to the λ -strong convexity of Ω [6, Proposition 3], and thus the self-bounding property holds with $M = 1/\lambda$. Below are two examples of the Fenchel–Young loss.

Logistic loss. The logistic loss can be seen as a Fenchel–Young loss. Consider the classification problem with K classes. Let $d = K$ and $\rho(y) = \mathbf{e}^y$ for $y \in \mathcal{Y} = [K]$ and $\mathcal{C} = \Delta^K$. If we adopt the negative Shannon entropy, $\Omega(\boldsymbol{\mu}) = \sum_{y \in \mathcal{Y}} \mu_y \ln \mu_y$ for $\boldsymbol{\mu} \in \Delta^K$, as a regularizer, the resulting Fenchel–Young loss is the logistic loss [7, Section 4.3]:

$$L_t(\mathbf{W}) = L_\Omega(\mathbf{W}\mathbf{x}_t, y_t) = \ln \sum_{y \in \mathcal{Y}} \exp(\theta_y) - \theta_{y_t},$$

where $\boldsymbol{\theta} = \mathbf{W}\mathbf{x}_t$ and $\theta_y = \langle \mathbf{e}^y, \mathbf{W}\mathbf{x}_t \rangle$ for $y \in \mathcal{Y}$. In this case, the regularized prediction, ρ_Ω , equals the softmax function. The negative Shannon entropy is 1-strongly convex on Δ^K with respect to the ℓ_1 -norm, and hence with respect to the ℓ_2 -norm. Thus, the self-bounding property holds with $M = 1$. Note that in some cases the base of the logarithm in the logistic loss is not Euler’s number e but rather 2 or K [31, 32, 28]; accordingly, the Lipschitz constant and the value of M also change.

SparseMAP loss. The SparseMAP loss, proposed by Niculae et al. [22], is another example of Fenchel–Young losses that applies to general structured prediction problems. Let $\mathcal{Y} = [K]$ be a finite set of labels and $\mathcal{C} = \text{conv}(\{\rho(y) \in \mathbb{R}^d : y \in \mathcal{Y}\})$. Let

$$\Omega(\boldsymbol{\mu}) = \begin{cases} \frac{1}{2} \|\boldsymbol{\mu}\|_2^2 & \text{if } \boldsymbol{\mu} \in \mathcal{C}, \\ +\infty & \text{otherwise.} \end{cases}$$

The resulting Fenchel–Young loss, $\boldsymbol{\theta} \mapsto L_\Omega(\boldsymbol{\theta}, y)$, is called the SparseMAP loss, whose regularized prediction $\rho_\Omega(\boldsymbol{\theta}) = \arg \max \{ \langle \boldsymbol{\theta}, \boldsymbol{\mu} \rangle - \Omega(\boldsymbol{\mu}) : \boldsymbol{\mu} \in \mathcal{C} \}$ tends to have a sparse support. Since Ω is 1-strongly convex with respect to the ℓ_2 -norm on \mathcal{C} , L_Ω is 1-smooth and hence self-bounding with $M = 1$.

B.3 Convolutional Fenchel–Young Loss: The Ranking Case

The definition of the convolutional Fenchel–Young loss is given in Definition 4.1, which satisfies the self-bounding property similarly to Fenchel–Young losses. Below, we discuss the computational aspect when applying our method with the convolutional Fenchel–Young loss to the label ranking problem with the NDCG loss in Appendix A.3. Recall that the convolutional Fenchel–Young loss is an instance of the Fenchel–Young loss generated by $\Omega_\tau = \Omega + \tau$, where $\tau(\boldsymbol{\mu}) = -\min_{\hat{y} \in \hat{\mathcal{Y}}} \langle \boldsymbol{\mu}, \ell^\rho(\hat{y}) \rangle$. As in Assumption 4.2, we assume that Ω is a λ -strongly convex function with $\text{dom}(\Omega) = \mathcal{C}$, e.g., $\Omega = \frac{\lambda}{2} \|\cdot\|_2^2 + \mathbb{I}_\mathcal{C}$, where $\mathbb{I}_\mathcal{C}(\boldsymbol{\mu}) = +\infty$ if $\boldsymbol{\mu} \notin \mathcal{C}$ and 0 otherwise.

When applying our method, we need to (i) compute the gradient of the convolutional Fenchel–Young loss $L_{\Omega_\tau}(\boldsymbol{\theta}, y)$ with respect to $\boldsymbol{\theta}$ and (ii) draw a sample $\hat{y} \in \hat{\mathcal{Y}}$ from the decoding distribution $\boldsymbol{\pi}(\boldsymbol{\theta}) \in \arg \min_{\boldsymbol{\pi} \in \Delta^N} \Omega^*(\boldsymbol{\theta} + \mathcal{L}^\rho \boldsymbol{\pi})$ to convert $\boldsymbol{\theta} \in \mathbb{R}^d$ into a prediction $\hat{y} \in \hat{\mathcal{Y}}$. Both can be addressed through the following problem, as discussed in Cao et al. [10, Section 5]:

$$\min_{\boldsymbol{\nu} \in \mathcal{V}} \Omega^*(\boldsymbol{\theta} + \boldsymbol{\nu}) \quad \text{where } \mathcal{V} = \text{conv}(\{\ell^\rho(\hat{y}) : \hat{y} \in \hat{\mathcal{Y}}\}). \quad (9)$$

Thanks to Danskin’s theorem [16], we can compute the gradient of Ω^* at any $\boldsymbol{\xi} \in \mathbb{R}^d$ as $\nabla \Omega^*(\boldsymbol{\xi}) = \arg \max_{\boldsymbol{\mu} \in \mathbb{R}^d} \langle \boldsymbol{\xi}, \boldsymbol{\mu} \rangle - \Omega(\boldsymbol{\mu})$. Thus, we can solve this problem by using first-order methods.

In the ranking problem in Appendix A.3, $\hat{\mathcal{Y}}$ is the set of permutations of $[d]$, and the loss vector of the NDCG loss is given by $\ell^\rho(\hat{y}) = (w_{\hat{y}(1)}, \dots, w_{\hat{y}(d)})^\top$, where $w_1, \dots, w_d \geq 0$ are the weights of d documents. Let $\mathbf{P}_{\hat{y}} \in \{0, 1\}^{d \times d}$ denote the permutation matrix corresponding to $\hat{y} \in \hat{\mathcal{Y}}$. Then, we have $\ell^\rho(\hat{y}) = \mathbf{P}_{\hat{y}} \mathbf{w}$, where $\mathbf{w} = (w_1, \dots, w_d)^\top$. Consequently, problem (9) can be rewritten as

$$\min_{\mathbf{P} \in \mathcal{B}} \Omega^*(\boldsymbol{\theta} + \mathbf{P} \mathbf{w}) \quad \text{where } \mathcal{B} = \{\mathbf{P} \in \mathbb{R}^{d \times d} : \mathbf{P}\mathbf{1} = \mathbf{1}, \mathbf{P}^\top \mathbf{1} = \mathbf{1}, \mathbf{P} \geq 0\}. \quad (10)$$

The set \mathcal{B} is the so-called Birkhoff polytope, which is the convex hull of the permutation matrices. Consider solving problem (10) with a Frank–Wolfe-type algorithm (e.g., [20, 17]). By using techniques for implementing

Carathéodory's theorem [3, 4], we can obtain a solution to problem (10) as a convex combination of $d^2 + 1$ vertices, each of which represents a permutation \hat{y} . Let $\mathbf{P}^* \in \mathcal{B}$ be an optimal solution to problem (10), $\hat{\mathcal{Y}}^* \subseteq \hat{\mathcal{Y}}$ the set of permutations with non-zero coefficients in the convex combination, and $\{\pi_{\hat{y}}^*\}_{\hat{y} \in \hat{\mathcal{Y}}^*}$ the non-zero coefficients, i.e., $\mathbf{P}^* = \sum_{\hat{y} \in \hat{\mathcal{Y}}^*} \pi_{\hat{y}}^* \mathbf{P}_{\hat{y}}$. Then, the decoding distribution $\boldsymbol{\pi}(\boldsymbol{\theta})$ is obtained by setting $\pi_{\hat{y}}(\boldsymbol{\theta})$ to $\pi_{\hat{y}}^*$ for $\hat{y} \in \hat{\mathcal{Y}}^*$ and 0 otherwise. By the envelope theorem [10, Lemma 12], the gradient required in (i) can be written as $\nabla \Omega^*(\boldsymbol{\theta} + \mathcal{L}^P \boldsymbol{\pi}(\boldsymbol{\theta})) - \boldsymbol{\rho}(y)$, which we can compute as $\nabla \Omega^*(\boldsymbol{\theta} + \mathbf{P}^* \mathbf{w}) - \boldsymbol{\rho}(y)$, where $\nabla \Omega^*(\boldsymbol{\theta} + \mathbf{P}^* \mathbf{w}) = \arg \max_{\boldsymbol{\mu} \in \mathbb{R}^d} \langle \boldsymbol{\theta} + \mathbf{P}^* \mathbf{w}, \boldsymbol{\mu} \rangle - \Omega(\boldsymbol{\mu})$ by Danskin's theorem. Regarding (ii), we can efficiently sample from $\boldsymbol{\pi}(\boldsymbol{\theta})$ by drawing $\hat{y} \in \hat{\mathcal{Y}}^*$ following the distribution $\boldsymbol{\pi}^*$ on $\hat{\mathcal{Y}}^*$.

While we have discussed the case of the ranking problem for concreteness, a similar approach works when a polyhedral representation of \mathcal{V} , like the Birkhoff polytope, is available.

C Discussion on the Hinge Loss

In Van der Hoeven [31] and Van der Hoeven et al. [32], the hinge loss for multiclass classification is introduced as a surrogate loss satisfying the self-bounding property (Assumption 3.3). However, we show that their hinge loss is discontinuous, hence non-convex, and that the standard hinge loss [14] is not self-bounding. Therefore, the hinge loss is not a valid surrogate loss for exploiting the surrogate gap.

Consider online classification with $K = d$ classes. For each round t , the hinge loss used in Van der Hoeven [31] and Van der Hoeven et al. [32] is defined with parameter $\kappa \in [0, 1]$ as follows:

$$L_t(\mathbf{W}) = L(\mathbf{W} \mathbf{x}_t, y_t) = \begin{cases} \max\{1 - m_t(\mathbf{W}, y_t), 0\} & \text{if } y_t^* \neq y_t \text{ or } m_t^*(\mathbf{W}) \leq \kappa, \\ 0 & \text{if } y_t^* = y_t \text{ and } m_t^*(\mathbf{W}) > \kappa, \end{cases}$$

where

$$\begin{aligned} m_t(\mathbf{W}, y) &= \langle \mathbf{e}^y, \mathbf{W} \mathbf{x}_t \rangle - \max_{y' \neq y} \langle \mathbf{e}^{y'}, \mathbf{W} \mathbf{x}_t \rangle, \\ m_t^*(\mathbf{W}) &= \max_{y \in \mathcal{Y}} m_t(\mathbf{W}, y), \quad \text{and} \\ y_t^* &\in \arg \max_{y \in \mathcal{Y}} \langle \mathbf{e}^y, \mathbf{W} \mathbf{x}_t \rangle. \end{aligned}$$

Let $\tilde{y}_t \in \arg \max_{y \neq y_t} \langle \mathbf{e}^y, \mathbf{W} \mathbf{x}_t \rangle$. A subgradient of L_t at \mathbf{W} is given by

$$\mathbf{G}_t(\mathbf{W}) = \begin{cases} (\mathbf{e}^{\tilde{y}_t} - \mathbf{e}^{y_t}) \mathbf{x}_t^\top & \text{if } y_t^* \neq y_t \text{ or } m_t^*(\mathbf{W}) \leq \kappa, \\ 0 & \text{if } y_t^* = y_t \text{ and } m_t^*(\mathbf{W}) > \kappa, \end{cases}$$

where 0 means the all-zero matrix.

Below, we argue that the hinge loss with $\kappa < 1$ is discontinuous (though self-bounding) and that the hinge loss with $\kappa = 1$ is not self-bounding (though convex).

The case of $\kappa < 1$. Note that we have $m_t(\mathbf{W}, y_t) \leq m_t^*(\mathbf{W})$. Thus, when $\kappa < 1$, $L_t(\mathbf{W})$ viewed as a univariate function of $m_t(\mathbf{W}, y_t)$ is discontinuous, where $L_t(\mathbf{W}) = 1 - m_t(\mathbf{W}, y_t) \geq 1 - \kappa$ for $m_t(\mathbf{W}, y_t) \leq \kappa$ and $L_t(\mathbf{W}) = 0$ for $m_t(\mathbf{W}, y_t) > \kappa$. This implies that $L_t(\mathbf{W})$ viewed as a function of $\mathbf{W} \in \mathcal{W}$ is discontinuous at the region where $m_t(\mathbf{W}, y_t) = \kappa$ holds. The parameter, κ , is set to $1/K$ in Van der Hoeven [31] and to $1/2$ in Van der Hoeven et al. [32]; therefore, the hinge loss used in their work is discontinuous, hence non-convex.

The case of $\kappa = 1$. The choice of $\kappa = 1$ corresponds to the standard convex hinge loss for multiclass classification. However, this is not self-bounding. Suppose $\|\mathbf{x}_t\|_2 = 1$. Then, if $y_t^* = y_t$ and $m_t^*(\mathbf{W}) \leq \kappa = 1$, we have $\|\mathbf{G}_t(\mathbf{W})\|_F^2 = 2\|\mathbf{x}_t\|_2^2 = 2$. On the other hand, the loss value, $L_t(\mathbf{W}) = 1 - m_t^*(\mathbf{W})$, can be arbitrarily close to zero as $m_t^*(\mathbf{W})$ approaches $\kappa = 1$, preventing us from ensuring $\|\mathbf{G}_t(\mathbf{W})\|_F^2 \lesssim L_t(\mathbf{W})$. Therefore, the hinge loss with $\kappa = 1$ is not self-bounding.

D Proof of Proposition 2.4

Proof. By the standard analysis of OGD (e.g., [23, Theorem 2.13]), for any t and $\mathbf{U}_t \in \mathcal{W}$, we have

$$L_t(\mathbf{W}_t) - L_t(\mathbf{U}_t) \leq \frac{\|\mathbf{W}_t - \mathbf{U}_t\|_{\text{F}}^2 - \|\mathbf{W}_{t+1} - \mathbf{U}_t\|_{\text{F}}^2}{2\eta_t} + \frac{\eta_t}{2} \|\mathbf{G}_t\|_{\text{F}}^2.$$

Taking summation over t , we obtain

$$\sum_{t=1}^T (L_t(\mathbf{W}_t) - L_t(\mathbf{U}_t)) \leq \underbrace{\sum_{t=1}^T \frac{\|\mathbf{W}_t - \mathbf{U}_t\|_{\text{F}}^2 - \|\mathbf{W}_{t+1} - \mathbf{U}_t\|_{\text{F}}^2}{2\eta_t}}_{(\text{A})} + \sum_{t=1}^T \frac{\eta_t}{2} \|\mathbf{G}_t\|_{\text{F}}^2,$$

where we define $\mathbf{W}_{T+1} = \mathbf{W}_T$. Also, we define $\mathbf{U}_{T+1} = \mathbf{U}_T$ for convenience. For $t = 1, \dots, T$, it holds that

$$\begin{aligned} \|\mathbf{W}_{t+1} - \mathbf{U}_t\|_{\text{F}}^2 &= \|\mathbf{W}_{t+1} - \mathbf{U}_{t+1}\|_{\text{F}}^2 + \|\mathbf{U}_{t+1} - \mathbf{U}_t\|_{\text{F}}^2 + 2\langle \mathbf{W}_{t+1} - \mathbf{U}_{t+1}, \mathbf{U}_{t+1} - \mathbf{U}_t \rangle \\ &\geq \|\mathbf{W}_{t+1} - \mathbf{U}_{t+1}\|_{\text{F}}^2 + 2\langle \mathbf{W}_{t+1} - \mathbf{U}_{t+1}, \mathbf{U}_{t+1} - \mathbf{U}_t \rangle \quad \text{Ignoring } \|\mathbf{U}_{t+1} - \mathbf{U}_t\|_{\text{F}}^2 \geq 0 \\ &\geq \|\mathbf{W}_{t+1} - \mathbf{U}_{t+1}\|_{\text{F}}^2 - 2D\|\mathbf{U}_{t+1} - \mathbf{U}_t\|_{\text{F}}. \quad \text{Cauchy-Schwarz and } \|\mathbf{W}_{t+1} - \mathbf{U}_{t+1}\|_{\text{F}} \leq D \end{aligned}$$

Therefore, we have

$$(\text{A}) \leq \underbrace{\sum_{t=1}^T \frac{\|\mathbf{W}_t - \mathbf{U}_t\|_{\text{F}}^2 - \|\mathbf{W}_{t+1} - \mathbf{U}_{t+1}\|_{\text{F}}^2}{2\eta_t}}_{(\text{B})} + \underbrace{\sum_{t=1}^T \frac{D}{\eta_t} \|\mathbf{U}_{t+1} - \mathbf{U}_t\|_{\text{F}}}_{(\text{C})}.$$

Since η_t is non-increasing, $\eta_t \geq \eta_T$ holds, and thus (C) is at most $\frac{D}{\eta_T} P_T$. We bound (B) from above as follows:

$$\begin{aligned} (\text{B}) &= \frac{\|\mathbf{W}_1 - \mathbf{U}_1\|_{\text{F}}^2}{2\eta_1} + \frac{1}{2} \sum_{t=2}^T \left(\frac{1}{\eta_t} - \frac{1}{\eta_{t-1}} \right) \|\mathbf{W}_t - \mathbf{U}_t\|_{\text{F}}^2 - \frac{\|\mathbf{W}_{T+1} - \mathbf{U}_{T+1}\|_{\text{F}}^2}{2\eta_T} \quad \text{Summation by parts} \\ &\leq \frac{\|\mathbf{W}_1 - \mathbf{U}_1\|_{\text{F}}^2}{2\eta_1} + \frac{1}{2} \sum_{t=2}^T \left(\frac{1}{\eta_t} - \frac{1}{\eta_{t-1}} \right) \|\mathbf{W}_t - \mathbf{U}_t\|_{\text{F}}^2 \quad \text{Ignoring the last term} \\ &\leq \frac{D^2}{2\eta_1} + \frac{D^2}{2} \sum_{t=2}^T \left(\frac{1}{\eta_t} - \frac{1}{\eta_{t-1}} \right) \quad \eta_{t-1} \geq \eta_t \text{ and } \|\mathbf{W}_t - \mathbf{U}_t\|_{\text{F}} \leq D \\ &= \frac{D^2}{2\eta_1} + \frac{D^2}{2} \left(\frac{1}{\eta_T} - \frac{1}{\eta_1} \right) \quad \text{Telescoping} \\ &= \frac{D^2}{2\eta_T}. \end{aligned}$$

Therefore, we can bound (A) from above by $\frac{D}{\eta_T} \left(\frac{D}{2} + P_T \right)$, obtaining the desired bound. \square

E Numerical Experiments

We experimentally evaluate the performance of our proposed Polyak-style learning rate (see Section 3.4) in comparison to other learning rates. Experiments were conducted on Google Colab with an AMD EPYC 7B12 CPU, 12 GB RAM, running Ubuntu 22.04.

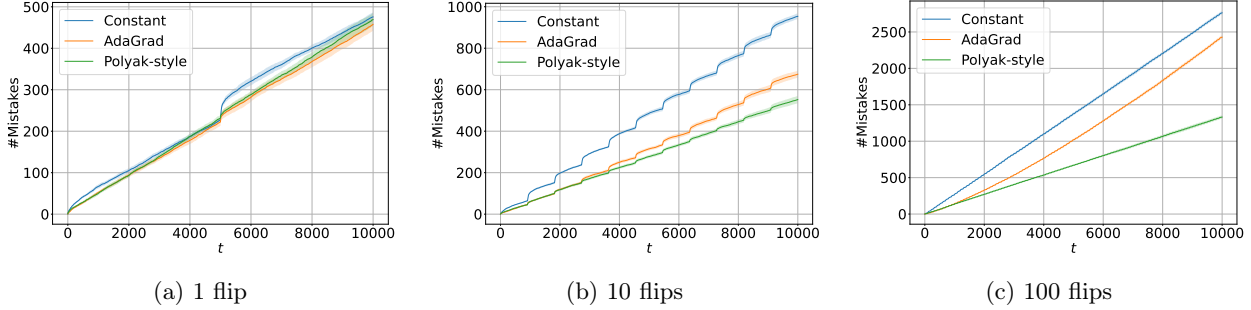


Figure 1: Experimental results for different learning rates under varying numbers of label flips.

Setup. We consider online binary classification over $T = 10,000$ rounds with the logistic surrogate loss:

$$L(\mathbf{w}; \mathbf{x}_t, y_t) = \log_2(1 + \exp(-y_t \langle \mathbf{w}, \mathbf{x}_t \rangle)),$$

where $\mathbf{w} \in \mathbb{R}^2$ is a linear estimator (expressed as a vector, rather than a matrix \mathbf{W}), $y_t \in \{-1, +1\}$ indicates a binary label, and $\mathbf{x}_t \in \mathbb{R}^2$ is an input feature vector drawn uniformly from the two dimensional unit sphere. This loss function satisfies the self-bounding property in Assumption 3.3 with $M = \frac{1}{\ln 2}$ [31, Lemma 2]. We define a reference vector $\mathbf{u} = \frac{1}{\sqrt{2}}(1, 1)^\top$. In the stationary environment, labels are given by $y_t = +1$ if $\langle \mathbf{u}, \mathbf{x}_t \rangle \geq 0$ and -1 otherwise. Non-stationarity is simulated by introducing segment-wise label flips: the number of flips is set to $\{1, 10, 100\}$, and at each flip all labels are multiplied by -1 . Consequently, the true estimator in each segment alternates between \mathbf{u} and $-\mathbf{u}$. We run OGD with projection onto an ℓ_2 -ball of diameter $D = 20$. Although the true directions, \mathbf{u} and $-\mathbf{u}$, lie in the unit ball, their exact scale is typically unknown a priori. We thus adopt a larger diameter of $D = 20$ to reflect this uncertainty. The decoding method used in this section is that of Van der Hoeven et al. [32]. This decoding approach, when applied to binary classification, yields a surrogate gap of $\alpha = 1/K = 1/2$. As the evaluation metric, we report the cumulative 0-1 loss (number of mistakes). Each configuration is repeated for 10 independent trials, and we plot the mean and the 95% confidence intervals.

Methods. We compare the following learning rates:

- **Constant:** a fixed value of $\eta_t = \frac{\alpha}{M} = \frac{1}{2\ln 2}$, which satisfies (4) in Theorem 3.4. This approach was adopted by Van der Hoeven [31] and Sakaue et al. [28].
- **AdaGrad:** a standard adaptive learning rate of $\eta_t = \frac{D}{\sqrt{2 \sum_{s=1}^t \|\nabla L(\mathbf{w}_s; \mathbf{x}_s, y_s)\|_2^2}}$ (see e.g., [23, Theorem 4.25]). This does not necessarily satisfy (4) in Theorem 3.4.
- **Polyak-style:** our proposed learning rate inspired by Polyak’s rule, which satisfies (4) in Theorem 3.4.

Results. Figure 1 summarizes the results: the curves of the cumulative number of mistakes with 95% confidence intervals over 10 independent trials. For the “1 flip” setting (nearly stationary), “Polyak-style” performs slightly worse than AdaGrad, yet remains competitive. For “10 flips” (moderately non-stationary), the constant learning rate performs worst; AdaGrad and Polyak-style are close, with Polyak-style slightly better and robust to label flips. For “100 flips” (highly non-stationary), the constant learning rate again performs worst, and AdaGrad is clearly worse than Polyak-style. In summary, the Polyak-style learning rate consistently achieves competitive or superior performance, with its advantage becoming more evident as the level of non-stationarity increases.

F Missing Proofs and Discussion in Section 4

F.1 Proof of Lemma 4.3

Proof. As shown in Cao et al. [10, Lemma 8], the conjugacy of addition and infimal convolution implies $\Omega_\tau^*(\boldsymbol{\theta}) = (\Omega + \tau)^*(\boldsymbol{\theta}) = \inf \{ \Omega^*(\boldsymbol{\theta} - \boldsymbol{\theta}') + \tau^*(\boldsymbol{\theta}') : \boldsymbol{\theta}' \in \mathbb{R}^d \} = \Omega^*(\boldsymbol{\theta} + \mathcal{L}^\rho \boldsymbol{\pi}(\boldsymbol{\theta}))$. Thus, we have

$$\begin{aligned} L_{\Omega_\tau}(\boldsymbol{\theta}, y) &= \Omega^*(\boldsymbol{\theta} + \mathcal{L}^\rho \boldsymbol{\pi}(\boldsymbol{\theta})) + \Omega(\boldsymbol{\rho}(y)) + \tau(\boldsymbol{\rho}(y)) - \langle \boldsymbol{\theta}, \boldsymbol{\rho}(y) \rangle \\ &= \Omega^*(\boldsymbol{\theta} + \mathcal{L}^\rho \boldsymbol{\pi}(\boldsymbol{\theta})) + \Omega(\boldsymbol{\rho}(y)) - \langle \boldsymbol{\theta} + \mathcal{L}^\rho \boldsymbol{\pi}(\boldsymbol{\theta}), \boldsymbol{\rho}(y) \rangle + \langle \mathcal{L}^\rho \boldsymbol{\pi}(\boldsymbol{\theta}), \boldsymbol{\rho}(y) \rangle + \tau(\boldsymbol{\rho}(y)) \\ &= L_\Omega(\boldsymbol{\theta} + \mathcal{L}^\rho \boldsymbol{\pi}(\boldsymbol{\theta}), y) + \langle \mathcal{L}^\rho \boldsymbol{\pi}(\boldsymbol{\theta}), \boldsymbol{\rho}(y) \rangle + \tau(\boldsymbol{\rho}(y)), \end{aligned}$$

where the last equality comes from the definition of the Fenchel–Young loss with the regularizer Ω . Therefore, it remains to show $\langle \mathcal{L}^\rho \boldsymbol{\pi}(\boldsymbol{\theta}), \boldsymbol{\rho}(y) \rangle + \tau(\boldsymbol{\rho}(y)) = \mathbb{E}_{\hat{y} \sim \boldsymbol{\pi}(\boldsymbol{\theta})}[\ell(\hat{y}, y)]$. From $\min_{\hat{y} \in \hat{\mathcal{Y}}} \ell(\hat{y}, y) = 0$ in Assumption 2.2 and $-\min_{\hat{y} \in \hat{\mathcal{Y}}} \langle \boldsymbol{\rho}(y), \boldsymbol{\ell}^\rho(\hat{y}) \rangle = \tau(\boldsymbol{\rho}(y))$ in Definition 4.1, we have

$$\min_{\hat{y} \in \hat{\mathcal{Y}}} \ell(\hat{y}, y) = \min_{\hat{y} \in \hat{\mathcal{Y}}} \langle \boldsymbol{\rho}(y), \boldsymbol{\ell}^\rho(\hat{y}) \rangle + c(y) = -\tau(\boldsymbol{\rho}(y)) + c(y) = 0,$$

hence $\tau(\boldsymbol{\rho}(y)) = c(y)$. Therefore, we obtain

$$\langle \mathcal{L}^\rho \boldsymbol{\pi}(\boldsymbol{\theta}), \boldsymbol{\rho}(y) \rangle + \tau(\boldsymbol{\rho}(y)) = \langle \mathcal{L}^\rho \boldsymbol{\pi}(\boldsymbol{\theta}), \boldsymbol{\rho}(y) \rangle + c(y) = \sum_{\hat{y} \in \hat{\mathcal{Y}}} \pi_{\hat{y}}(\boldsymbol{\theta}) (\langle \boldsymbol{\rho}(y), \boldsymbol{\ell}^\rho(\hat{y}) \rangle + c(y)) = \mathbb{E}_{\hat{y} \sim \boldsymbol{\pi}(\boldsymbol{\theta})}[\ell(\hat{y}, y)],$$

as desired. \square

F.2 Discussion on the Connection to Cao et al. [10]

We discuss the connection between Lemma 4.3 and the excess risk analysis of Cao et al. [10]. In the proof of Cao et al. [10, Lemma 14], for any $\boldsymbol{\eta} \in \Delta^K$ and $\boldsymbol{\theta} \in \mathbb{R}^d$, it has been shown that

$$\begin{aligned} \mathbb{E}_{y \sim \boldsymbol{\eta}}[L_{\Omega_\tau}(\boldsymbol{\theta}, y)] &- \inf_{\boldsymbol{\theta} \in \mathbb{R}^d} \mathbb{E}_{y \sim \boldsymbol{\eta}}[L_{\Omega_\tau}(\boldsymbol{\theta}, y)] \\ &= L_\Omega(\boldsymbol{\theta} + \mathcal{L}^\rho \boldsymbol{\pi}(\boldsymbol{\theta}), y) + \mathbb{E}_{\hat{y} \sim \boldsymbol{\pi}(\boldsymbol{\theta})}[\mathbb{E}_{y \sim \boldsymbol{\eta}}[\ell(\hat{y}, y)]] - \min_{\hat{y} \in \hat{\mathcal{Y}}} \mathbb{E}_{y \sim \boldsymbol{\eta}}[\ell(\hat{y}, y)] \end{aligned}$$

holds. The proof of this equality is built on $\Omega_\tau^*(\boldsymbol{\theta}) = \Omega^*(\boldsymbol{\theta} + \mathcal{L}^\rho \boldsymbol{\pi}(\boldsymbol{\theta}))$ [10, Lemma 8], as with our proof of Lemma 4.3. Then, by ignoring $L_\Omega(\boldsymbol{\theta} + \mathcal{L}^\rho \boldsymbol{\pi}(\boldsymbol{\theta}), y) \geq 0$, the authors obtained

$$\mathbb{E}_{\hat{y} \sim \boldsymbol{\pi}(\boldsymbol{\theta})}[\mathbb{E}_{y \sim \boldsymbol{\eta}}[\ell(\hat{y}, y)]] - \min_{\hat{y} \in \hat{\mathcal{Y}}} \mathbb{E}_{y \sim \boldsymbol{\eta}}[\ell(\hat{y}, y)] \leq \mathbb{E}_{y \sim \boldsymbol{\eta}}[L_{\Omega_\tau}(\boldsymbol{\theta}, y)] - \inf_{\boldsymbol{\theta} \in \mathbb{R}^d} \mathbb{E}_{y \sim \boldsymbol{\eta}}[L_{\Omega_\tau}(\boldsymbol{\theta}, y)],$$

namely, a linear bound on the target excess risk by the surrogate excess risk. At this point, the proof of our Lemma 4.3 deviates from their original proof. First, we do not ignore $L_\Omega(\boldsymbol{\theta} + \mathcal{L}^\rho \boldsymbol{\pi}(\boldsymbol{\theta}), y) \geq 0$, which plays a crucial role in our analysis through Lemma 4.4. Second, we are interested in evaluating the target and surrogate losses on ground-truth y_t , rather than on a distribution $\boldsymbol{\eta}$. Therefore, we can simplify the expression by focusing on the case of $\boldsymbol{\eta} = \mathbf{e}^y$ for ground-truth $y \in \mathcal{Y}$. This indeed implies $\inf_{\boldsymbol{\theta} \in \mathbb{R}^d} \mathbb{E}_{y \sim \boldsymbol{\eta}}[L_{\Omega_\tau}(\boldsymbol{\theta}, y)] = 0$ and $\min_{\hat{y} \in \hat{\mathcal{Y}}} \mathbb{E}_{y \sim \boldsymbol{\eta}}[\ell(\hat{y}, y)] = 0$ under Assumption 2.2. Consequently, we obtain the target–surrogate relation in Lemma 4.3:

$$L_{\Omega_\tau}(\boldsymbol{\theta}, y) = L_\Omega(\boldsymbol{\theta} + \mathcal{L}^\rho \boldsymbol{\pi}(\boldsymbol{\theta}), y) + \mathbb{E}_{\hat{y} \sim \boldsymbol{\pi}(\boldsymbol{\theta})}[\ell(\hat{y}, y)].$$

As above, while our Lemma 4.3 is built on a similar analysis to that of Cao et al. [10], it is tailored for our purpose of deriving the “small-surrogate-loss + path-length” bound.

F.3 Proof of Lemma 4.4

Proof. From $\text{dom}(\Omega) = \mathcal{C}$ and Danskin's theorem [16], we have $\nabla\Omega^*(\boldsymbol{\theta} + \mathcal{L}^\rho\boldsymbol{\pi}(\boldsymbol{\theta})) = \arg\max_{\boldsymbol{\mu} \in \mathcal{C}}\{\langle\boldsymbol{\theta} + \mathcal{L}^\rho\boldsymbol{\pi}(\boldsymbol{\theta}), \boldsymbol{\mu}\rangle - \Omega(\boldsymbol{\mu})\}$.⁹ Since Ω is λ -strongly convex over $\mathcal{C} = \text{conv}(\{\boldsymbol{\rho}(y) \in \mathbb{R}^d : y \in \mathcal{Y}\})$, the quadratic lower bound on the (standard) Fenchel–Young loss [6, Proposition 3] implies

$$L_\Omega(\boldsymbol{\theta} + \mathcal{L}^\rho\boldsymbol{\pi}(\boldsymbol{\theta}), y) \geq \frac{\lambda}{2}\|\nabla\Omega^*(\boldsymbol{\theta} + \mathcal{L}^\rho\boldsymbol{\pi}(\boldsymbol{\theta})) - \boldsymbol{\rho}(y)\|_2^2.$$

Furthermore, the envelope theorem [10, Lemma 12] implies

$$\nabla L_{\Omega_\tau}(\boldsymbol{\theta}, y) = \nabla\Omega^*(\boldsymbol{\theta} + \mathcal{L}^\rho\boldsymbol{\pi}(\boldsymbol{\theta})) - \boldsymbol{\rho}(y).$$

Substituting this into the above quadratic lower bound yields the desired inequality. \square

G Proof of the Lower Bound

Proof of Theorem 5.1. Let T be a positive even integer, $K = d = 2$, $\mathcal{Y} = \hat{\mathcal{Y}} = \{-1, +1\}$, and $\mathbf{x}_t = (1, 0)^\top$ for $t = 1, \dots, T$. Set each ground-truth label y_t to -1 or $+1$ with equal probability. Then, any deterministic learner inevitably incurs $\mathbb{E}[Z_T] = T/2$, where $Z_T = \sum_{t=1}^T \ell(\hat{y}_t, y_t) = \sum_{t=1}^T \mathbb{1}_{\hat{y}_t \neq y_t}$. Thanks to celebrated Yao's principle [33], for any possibly randomized learner, there exists the worst-case instance such that $\mathbb{E}[Z_T] \geq T/2$, where the expectation is taken over the learner's possible randomness. Below, we let y_1, \dots, y_T be the labels of such an instance.

For the above instance, we design comparator sequences to show the claim. Let $\mathcal{W} = \{\mathbf{W} \in \mathbb{R}^{2 \times 2} : \|\mathbf{W}\|_{\text{F}} = 1\}$ be the domain and $\mathbf{U}_1, \dots, \mathbf{U}_T \in \mathcal{W}$ denote comparators. For convenience, let $\zeta_t = y_t \langle (+1, -1)^\top, \mathbf{U}_t \mathbf{x}_t \rangle$. Then, the smooth hinge loss (see Appendix B.1) satisfies

$$L_t(\mathbf{U}_t) = \begin{cases} 1 - 2\zeta_t & \text{if } \zeta_t \leq 0, \\ 1 - \zeta_t^2 & \text{if } 0 < \zeta_t < 1, \\ 0 & \text{if } 1 \leq \zeta_t. \end{cases}$$

We consider two comparator sequences defined as follows for $t = 1, \dots, T$:

$$(i) \quad \mathbf{U}_t = \frac{1}{2} \begin{bmatrix} +y_t & +1 \\ -y_t & +1 \end{bmatrix} \quad \text{and} \quad (ii) \quad \mathbf{U}_t = \frac{1}{2} \begin{bmatrix} +1 & +1 \\ -1 & +1 \end{bmatrix}.$$

In case (i), $\zeta_t = 1$ always holds and hence $F_T = 0$. As for the path length, $\|\mathbf{U}_t - \mathbf{U}_{t-1}\|_{\text{F}} \leq \sqrt{2}$ holds, and hence $P_T \leq \sqrt{2}(T-1)$. In case (ii), we have $P_T = 0$. As for the cumulative surrogate loss, we have either $\zeta_t = +1$ or -1 , hence $F_T \leq 3T$. Combining these with $\mathbb{E}[Z_T] \geq T/2$, we have

$$\mathbb{E}[Z_T] \geq T/2 \geq (P_T/\sqrt{2} + 1)/2 \quad \text{and} \quad F_T = 0 \quad \text{in case (i),} \quad \text{and} \quad (11)$$

$$\mathbb{E}[Z_T] \geq T/2 \geq F_T/6 \quad \text{and} \quad P_T = 0 \quad \text{in case (ii).} \quad (12)$$

We now consider establishing the claim with $\varepsilon_F = 0$ and $\varepsilon_P = \varepsilon > 0$. If $\mathbb{E}[Z_T] = O(F_T + P_T^{1-\varepsilon})$, it contradicts (11) since $P_T \lesssim T \lesssim \mathbb{E}[Z_T] \lesssim P_T^{1-\varepsilon}$ cannot not hold when T is large enough. Similarly, $\mathbb{E}[Z_T] = O(F_T^{1-\varepsilon} + P_T)$ contradicts (12). The case of $\varepsilon_F, \varepsilon_P > 0$ follows from these two claims. \square

⁹We assumed $\text{dom}(\Omega) = \mathcal{C}$ in Assumption 4.2 solely for ease of establishing this relation.